

Electrostatic correlations: from Plasma to Biology

Yan Levin

*Instituto de Física, Universidade Federal do Rio Grande do Sul
Caixa Postal 15051, CEP 91501-970, Porto Alegre, RS, Brazil
levin@if.ufrgs.br*

Abstract.

Electrostatic correlations play an important role in physics, chemistry and biology. In plasmas they lead to thermodynamic instability similar to the liquid-gas phase transition of simple molecular fluids. For charged colloidal suspensions the electrostatic correlations are responsible for screening and colloidal charge renormalization. In aqueous solutions containing multivalent counterions they can lead to charge inversion and flocculation. In biological systems the correlations account for the organization of cytoskeleton and the compaction of genetic material. In spite of their ubiquity, the true importance of electrostatic correlations has become fully appreciated only quite recently. In this paper, I will review the thermodynamic consequences of electrostatic correlations in a variety of systems ranging from classical plasmas to molecular biology.

Contents

1	Introduction	3
2	Electrolyte solutions	6
2.1	The Debye-Hückel theory	7
2.2	The Bjerrum association	11
3	Two-dimensional plasma and the Kosterlitz-Thouless transition	13
4	The one component plasma	16
4.1	Confined one component plasma	19
5	Asymmetric systems	23
5.1	Colloidal suspensions	23
5.2	Colloidal lattices	24
5.3	Density functional theory (<i>DFT</i>) for colloidal lattices	25
5.4	Charge Renormalization	29
5.5	Colloidal Fluid	31
6	Polyelectrolyte solutions	34
6.1	Manning condensation	35
6.2	Counterion Association	37
7	Multivalent counterions	41
7.1	Overcharging	42
7.2	Overcharging in electrolyte solutions	44
8	Like-charge attraction	50
8.1	Confined suspensions	50
8.2	Correlation-induced attraction	52
8.3	Counterion polarization	58
9	Conclusions	60
10	Acknowledgements	61

1. Introduction

Although the liquid state theorists have become quite accustomed to look at the correlation functions for simple and complex fluids, many of the thermodynamic consequences of correlations have not been fully appreciated. To some extent this is the result of the success of mean-field theories for simple fluids. The strategy of applying mean-field approximation to the many body problems goes all the way to the pioneering work of van der Waals on liquid-gas phase separation [1]. The success of this theory and its physical transparency has set the stage for future applications of mean-field ideas. These came in the form of the Curie-Weiss theory of magnetism [2] and the Gouy-Chapman [3, 4] theory of diffuse ionic layers.

There are, however, some very familiar systems in which the mean-field contribution to the free energy is purely zero. One such system is a classical two component plasma of positive and negative ions. In order for the thermodynamic limit to exist, charge neutrality constraint must be imposed. However, for a bulk charge neutral system the average electrostatic potential is zero, which means that the mean-field contribution to the total free energy also vanishes. Thus, the electrostatic free energy of a two component plasma is entirely due to positional correlations between positive and negative ions. At low temperatures, these correlations become so strong, as to lead to phase transition in which the plasma separates into two coexisting high and low density phases [5, 6].

Polar fluids provide another example of a system in which the electrostatic correlations strongly affect the thermodynamics. Perhaps the simplest model of a polar fluid is a system of dipolar hard spheres (*DHS*). The phase structure of *DHS* is quite interesting and deserves a separate review [7, 8, 9]. Here we shall confine our attention to the low density disordered fluid phase. Since the average electric field inside a dipolar fluid is zero, it is evident that the mean-field contribution to the free energy also vanishes, and all the non-trivial thermodynamics is, once again, the result of electrostatic correlations.

The thermodynamics of *DHS* is particularly tricky, because of the unscreened long range interactions. In fact the very existence of the thermodynamic limit for *DHS* has been proven only recently [10]. Nevertheless, it has been taken for granted that if the temperature is sufficiently low, the *DHS* will phase separate into coexisting liquid and gas phases. Indeed, all the theories have been predicting exactly this kind of behavior [11, 12]. It came, therefore, as a great surprise when the simulations in the early 90's failed to locate the anticipated liquid-gas critical point [13, 14, 15]. Instead as the temperature was lowered, the simulations found chains of aligned dipoles. The formation of weakly interacting chains, a consequence of strong positional and directional correlations between the dipolar particles, prevents the liquid-gas phase separation from taking place [16, 17, 18, 19].

Electrostatic correlations are also crucial in charged colloidal suspensions [20, 21]. In these systems the correlations come on two different levels. First, there are very strong positional correlations between the highly charged colloidal particles and

their counterions. These correlations lead to charge renormalization [22] and to screening of Coulomb interactions between the colloidal particles. In water with monovalent counterions, charge renormalization stabilizes colloidal suspension against phase separation [23, 24]. In the presence of multivalent counterions, however, the layers of condensed counterions on different colloids can become strongly correlated, leading to attraction between like-charged colloidal particles [25, 26] and to phase separation [27, 28].

A similar kind of behavior was also observed in a number of important biological systems. Thus, it was noted that like-charged macromolecules can attract each other in solutions containing multivalent counterions. This attraction manifests itself in *in vitro* formation of toroidal aggregates of concentrated DNA [29, 30], similar to the one found in bacteriophage heads [31], and in bundle formation of F-actin and tobacco mosaic virus [32]. A number of models have been suggested to explain these curious phenomena. The fundamental ingredient in all of these models are the electrostatic correlations [33, ?, 34].

Although the phenomena described above are quite complex, we can get a long way towards understanding them by considering some surprisingly simple models and theories. In fact, we shall demonstrate that a lot of the physics of electrostatic correlations is contained within the Debye-Hückel theory [35] introduced 80 years ago as a way of accounting for the unusual thermodynamic properties of strong electrolytes.

Consideration of only simple physical theories in this review is partially pedagogical, designed for a broad audience not necessarily familiar with the complex machinery of correlation functions and field theories of the modern statistical mechanics. For Coulomb systems there is, however, an additional benefit. It is often found that the more sophisticated theories fail when applied to strongly correlated charged fluids. For example, the field theoretic calculations of Netz and Orland [36] find that for charge asymmetric ($z : 1$) electrolytes the reduced critical temperature is a strongly increasing function of charge asymmetry. A completely opposite behavior is observed in computer simulations, the critical temperature decreases and the critical density increases with the charge asymmetry. In fact, the field theoretic predictions for the critical temperature of asymmetric electrolytes are so far-off that they have to be divided by a factor of six just to make them fit on the same graph (Fig. 1) with the results of simulations and of concurrent theories! The dramatic failure of field theoretic calculations can be attributed to their intrinsically perturbative nature. Similarly the integral equations, which have proven to be very successful for simple molecular fluids, fail to even converge for strongly asymmetric electrolytes. Furthermore, it has been known for a long time that the Hypernetted Chain Equation (HNC) which is often used to study the Coulomb systems [37], does not possess a true critical region, but only a “no solution zone” on the border of which compressibility goes to zero with a square root singularity [38, 39]. This is a completely wrong behavior, since the compressibility must diverge at the critical point. All these should be contrasted with the physically based Debye-Hückel-like theories, which are in qualitative and often in quantitative agreement with the

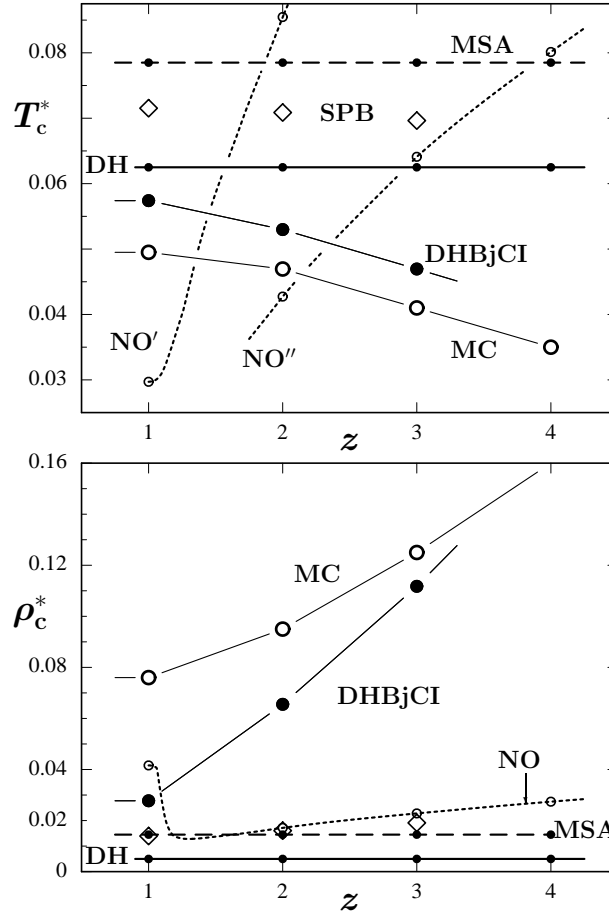


Figure 1. Estimates of the reduced critical temperature, T_c^* , and density, ρ_c^* , for the ($z : 1$), charge-asymmetric (but equisized) primitive model showing, as labeled, the predictions of pure Debye-Hückel theory (without hard cores), (b) the MSA, (c) the SPB approximation [40], (d) the Netz-Orland field-theoretic treatment [36] which, for T_c^* , have been divided by factors of 6 and 12 in order to bring them on to the plot (see labels NO' and NO'' respectively), and (e) the DHBjCI theory (following the Fisher-Levin approach [5, 6]). The large open circles for $z = 2$ and 3 represent, the Monte Carlo simulations of Panagiotopoulos and Fisher [41], while the estimate for $T_c^*(4)$ follows from Camp and Patey [42]. (After S. Banerjee and M. E. Fisher, to be published).

simulations and experiments, Fig. 1. For some important many body systems, however, the integral equations provide the most accurate results. For example, predictions for the electrostatic free energy of the one component plasma obtained using the *HNC* equation are in excellent agreement with the Monte Carlo simulations [43]. The integral equations were also the first to account for the correlation induced attraction between like-charged macromolecules [25, 44, 45]. In general, as long as one stays away from phase transitions, the integral equations provide one of the sharpest tools available to statistical physicist or chemist. Unfortunately, the approximations involved in constructing the integral equations are not very clear. There exists a great variety of closures to the Ornstein-

Zernike equation, each working well for a specific kind of problems. Because of their complexity, I will not talk about the integral equations in this review, referring the interested reader to the literature [46].

2. Electrolyte solutions

Since the work of Faraday early in the 19th century the flow of electricity has been associated with the movement of charged particles. The nature of ions (from Greek meaning wanderers), however, was not established. It was Arrhenius who in 1887, following the experimental work of van't Hoff on osmotic pressure of electrolyte solutions, proposed that when salts and acids are dissolved in water they become ionized [47]. Arrhenius suggested that in water $NaCl$ dissociates forming cations Na^+ and anions Cl^- . In the spirit of the mean-field theory introduced earlier by van der Waals [1], Arrhenius argued that since the anions and the cations are on average uniformly distributed throughout the solution, the average electrostatic potential inside the electrolyte is zero. He then concluded that on average there should not be any interaction between the ions, and the osmotic pressure of, say, 1M solution of $NaCl$ should be equivalent to the osmotic pressure of 2M solution of non-electrolyte. All the deviations from this simple rule Arrhenius attributed to the incomplete dissociation of electrolyte, which he then treated as a problem of chemical equilibrium, the thermodynamics of which has already been developed by Gibbs ten years earlier [48]. Soon, however, it became clear that while the theory was working well for weak electrolytes, such as Brønsted acids and bases, it failed for strong electrolytes such as $NaCl$ and HCl , which remained fully ionized even at fairly large concentrations. The disagreements between the theory and the experiment could not be accounted for by the postulate of incomplete dissociation. It appeared that there was a fundamental flaw in the theory advanced by Arrhenius, which relied on the mean-field assumption of non-interacting ions. The situation remained unclear for about 30 years, with various proposals made on how to incorporate the ionic interactions into the framework of Arrhenius' theory [48]. None of these have proven very successful at explaining the experimental measurements, until Debye and Hückel published their famous theory of strong electrolytes [35]. The fundamental insight of Debye and Hückel (DH) was to realize that although ions *on average* are randomly distributed, there exist strong positional correlations between the anions and cations. The depth of Debye's insight can be judged from the fact that he understood the role of electrostatic correlations significantly before the correlation functions became the standard tool of working physicists. Since so many of our results will be based on the fundamental ideas of Debye and Hückel, their theory will provide the starting point for our discussion of thermodynamics of electrostatic correlations.

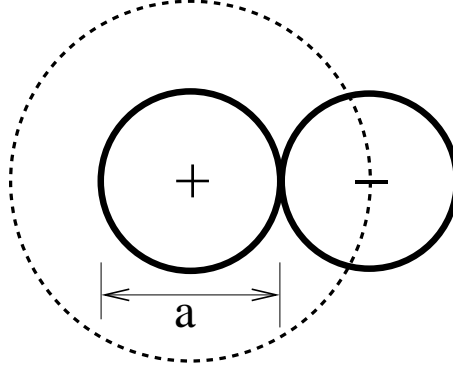


Figure 2. The configuration of closest approach between two oppositely charged ions. The dashed curve delimits the region into which no ions can penetrate, due to the hard core repulsion.

2.1. The Debye-Hückel theory

Consider the simplest model of an electrolyte solution confined to volume V . The N ions will be idealized as hard spheres of diameter a carrying charge $\pm q$ at their centers. The charge neutrality of solution requires that $N_+ = N_- = N/2$. The solvent will be modeled as a continuum of dielectric constant ϵ . Although the average potential inside the electrolyte is zero, there are strong positional correlations between the oppositely charged ions. It is convenient to work in spherical coordinates. To calculate the correlational contribution to the Helmholtz free energy, let us fix one ion of charge $+q$ at the origin $r = 0$ and see how the other ions will distribute around it, see Fig. 2. Inside the region $0 < r \leq a$ there are no other ions except for the one fixed at the origin, and the electrostatic potential $\phi(r)$ satisfies the Laplace equation,

$$\nabla^2 \phi = 0. \quad (1)$$

For $r > a$ the electrostatic potential satisfies the Poisson equation

$$\nabla^2 \phi = -\frac{4\pi}{\epsilon} \rho_q(r), \quad (2)$$

where the charge density can be expressed in terms of the charge-charge correlation functions $g_{++}(r) = g_{--}(r)$ and $g_{+-}(r) = g_{-+}(r)$

$$\rho_q(r) = q\rho_+g_{++}(r) - q\rho_-g_{+-}(r). \quad (3)$$

The average densities of positive and negative ions are $\rho_+ = N_+/V$, $\rho_- = N_-/V$; $\rho_+ = \rho_- = \rho/2$.

The correlation functions can be written in terms of the potential of mean force w_{ij}

$$g_{ij}(r) = e^{-\beta w_{ij}(r)}, \quad (4)$$

where $\beta = 1/k_B T$. The $w_{ij}(r)$ is the work required to bring ions i and j from infinity to separation r inside the electrolyte solution. In their paper Debye and Hückel made

an implicit approximation of replacing the potential of mean force by the electrostatic potential

$$w_{ij}(r) = q_j \phi_i(r) , \quad (5)$$

where q_j is the charge of j' th ion and $\phi_i(r)$ is the electrostatic potential at distance r from the ion i fixed at the origin $r = 0$. With this approximation, Eq.(2) reduces to the non-linear Poisson-Boltzmann equation (*PB*),

$$\nabla^2 \phi = -\frac{4\pi}{\epsilon} [q\rho_+ e^{-\beta q\phi} - q\rho_- e^{+\beta q\phi}] = \frac{4\pi\rho q}{\epsilon} \sinh(\beta q\phi) . \quad (6)$$

Debye and Hückel proceeded to linearize this equation. Technically, linearization is only valid if $\beta q\phi \ll 1$, however, being practically minded Debye and Hückel linearized first and worried about the consequences later. As was noted later by Onsager, linearization of Eq.(6) is a necessary step in order to produce a self-consistent theory[49]. The linearized Poisson-Boltzmann equation reduces to the Helmholtz equation

$$\nabla^2 \phi = \kappa^2 \phi , \quad (7)$$

where the inverse Debye length is

$$\xi_D^{-1} \equiv \kappa = \sqrt{\frac{4\pi q^2 \rho}{k_B T \epsilon}} . \quad (8)$$

The Laplace equation (1) for $r \leq a$ and the Helmholtz equation (7) for $r > a$ must be integrated, subject to the boundary condition of continuity of the electrostatic potential and the electric field across the boundary surface $r = a$. For $r \leq a$ the electrostatic potential is found to be

$$\phi_{<}(r) = \frac{q}{\epsilon r} - \frac{q\kappa}{\epsilon(1 + \kappa a)} , \quad (9)$$

while for $r > a$,

$$\phi_{>}(r) = \frac{q\theta(\kappa a)e^{-\kappa r}}{\epsilon r} , \quad \theta(x) = \frac{e^x}{(1+x)} . \quad (10)$$

Equation (10) shows that the electrostatic potential produced by the central charge is screened by the surrounding ionic cloud. Because of the hardcore repulsion the screening, however, appears only at distances larger than $r = a$. This accounts for the presence of the geometric factor $\theta(\kappa a)$ in Eq. (10). The screening of electrostatic interactions inside the electrolyte solutions and plasmas is responsible for the existence of the thermodynamic limit in these systems with extremely long range forces.

The electrostatic potential $\phi_{<}(r)$, Eq. (9), consists of two terms: the potential produced by the central ion $q/\epsilon r$, and the electrostatic potential induced by the surrounding ionic cloud,

$$\psi = -\frac{q\kappa}{\epsilon(1 + \kappa a)} . \quad (11)$$

The electrostatic free energy can now be obtained using the Debye charging process in which all ions are simultaneously charged from zero to their full charge,

$$F^{el} = Nq \int_0^1 d\lambda \psi(\lambda q) . \quad (12)$$

The calculation is very similar to the one used to obtain the electrostatic energy stored in a capacitor. While performing the charging it is important to remember that $\kappa(\lambda q) = \lambda \kappa(q)$. Defining the free energy density as $f = F/V$, the integral in Eq. (12) can be performed explicitly yielding

$$\beta f^{el} = \frac{\beta F^{el}}{V} = -\frac{1}{4\pi a^3} \left[\ln(\kappa a + 1) - \kappa a + \frac{(\kappa a)^2}{2} \right]. \quad (13)$$

For large dilutions Eq. (13) reduces to the famous Debye limiting law,

$$\beta f^{el} \approx -\frac{\kappa^3}{12\pi} \sim -\left(\frac{\rho}{T}\right)^{3/2}. \quad (14)$$

Given the free energy, the limiting laws for the osmotic pressure and activity can be easily found [6].

The free energy is not analytic at $\rho = 0$. The singularity at $\rho = 0$ is a consequence of long-range Coulomb interactions, which also manifest themselves in the divergence of the standard virial expansion [50]. The total free energy of the electrolyte F is the sum of the electrostatic Eq. (13), and the entropic contributions. The entropic contribution to the free energy arises from the integration over momentum degrees of freedom in the partition function, and is equivalent to the free energy of ideal gas,

$$\beta F^{ent} = N_+ \ln[\rho_+ \Lambda^3] - N_+ + N_- \ln[\rho_- \Lambda^3] - N_- = N \ln[\rho \Lambda^3/2] - N, \quad (15)$$

where the de Broglie thermal wavelength is

$$\Lambda = \frac{h}{\sqrt{2\pi m k_B T}}. \quad (16)$$

The osmotic pressure of the electrolyte is

$$P = -\left. \frac{\partial F}{\partial V} \right|_N, \quad (17)$$

which can also be expressed in terms of the Legendre transform of the negative free energy density $-f$ [6],

$$P = -f + \mu \rho, \quad (18)$$

where the chemical potential is

$$\mu = \frac{\partial F}{\partial N} = \frac{\partial f}{\partial \rho}. \quad (19)$$

It is a simple matter to see that below the critical temperature T_c the total free energy $F = F^{ent} + F^{el}$ fails to be a convex function of the electrolyte concentration. This implies the presence of a phase transition. Alternatively the phase separation can be observed from the appearance of a van der Waals loop in the osmotic pressure Eq. (18), below the critical temperature T_c . The critical parameters are determined by

$$\frac{\partial P}{\partial \rho} = 0, \quad (20)$$

$$\frac{\partial^2 P}{\partial \rho^2} = 0. \quad (21)$$

The coexistence curve can be obtained using the standard Maxwell construction. It is convenient to define the reduced temperature and density as $T^* = k_B T a \epsilon / q^2$ and $\rho^* = \rho a^3$. The critical point of the plasma, within the DH , is found to be located at [5, 6]

$$T_c^* = \frac{1}{16} , \quad (22)$$

and

$$\rho_c^* = \frac{1}{64\pi} . \quad (23)$$

It is interesting to note that at criticality $\kappa = 1/a$. This means that in spite of a very low concentration of electrolyte at the critical point, the screening remains very strong. We also observe that the reduced critical temperature for the electrolyte is almost an order of magnitude lower, than for systems in which particles interact by short-ranged isotropic potentials. Since the critical point within the DH theory occurs at extremely low density, we are justified in neglecting the excluded volume contribution to the total free energy.

Phase separation of an electrolyte or of a two component plasma is the result of an electrostatic instability arising from the strong positional correlations between the oppositely charged ions. This mechanism is very different from the one driving the phase separation in systems dominated by short ranged isotropic forces. In that case the thermodynamic instability is a consequence of the competition between the interparticle attraction and the hardcore repulsion.

The reduced temperature can be written as $T^* = a/\lambda_B$, where $\lambda_B = q^2/k_B T \epsilon$ is the Bjerrum length. For water at room temperature $\lambda_B \approx 7 \text{ \AA}$. This means that one would need ions of size less than 0.4 \AA , in order to observe phase separation at room temperature. This is clearly impossible since the minimum hydrated ionic size is about $2 - 4 \text{ \AA}$. Therefore, in order to see phase separation, one is required to look for solutions with λ_B on the order of 40 \AA or more. For water such large values of λ_B correspond to temperatures well below the freezing. An alternative is to work with organic solvents which have dielectric constants significantly lower than water. This was the strategy adopted by K.S. Pitzer in his studies of ionic criticality [51, 52, 53]. Pitzer used liquid salt triethyl-n-hexylammonium triethyl-n-hexylboride ($N_{2226}B_{2226}$) in diphenyl ether. With this he was able to observe the critical point at room temperature. Pitzer's work has provoked a lot of stimulating controversy because his measurements suggested that Coulombic criticality belonged to a new universality class. At first sight this might not seem very surprising, after all the Coulomb force is extremely long ranged. On further reflection the situation is not so clear. Although the bare interaction potential between any two ions is long ranged, inside the electrolyte solution it is screened by the surrounding particles, as can be seen from Eq. (10). The effective interaction potential, therefore, is short ranged, which should place the ionic criticality firmly in the Ising universality class. In fact all the theoretical arguments lead to this conclusion, which seems to be contradicted by the Pitzer's experiments. In principle, it is possible that

one has to be very close to the critical point before the Ising behavior becomes apparent. However, even this conclusion is hard to justify theoretically. Estimates of the Ginzburg criterion suggest that the width of the critical region for Coulombic criticality should be comparable to that of systems with short ranged isotropic interactions [5, 54]. The situation remains unclear.

An alternative to working with electrolyte solutions is to study molten salts, which are classical two component plasmas. In this case the dielectric constant can be taken to be that of vacuum, and ions are no longer hydrated. The reduced critical temperature $T^* = 1/16$ and the characteristic ionic diameter of about 2 \AA , imply that at criticality $\lambda_B \approx 30$, which means that the critical point for a molten salt is located at about $5000K$. It is, indeed, very hard to study critical phenomena at such high temperatures! It seems, therefore, that we are stuck with the low dielectric solvents. An alternative is the computer simulations, which are becoming sufficiently accurate to allow measurements of the critical exponents, at least for symmetric 1:1 electrolytes. Indeed the most recent simulations suggest that the Coulombic criticality belongs to the Ising universality class[55].

2.2. The Bjerrum association

The DH theory presented in the previous section was based on the linearization of the Poisson-Boltzmann equation. In view of the strong screening and the rapid decrease of the electrostatic potential away from the central ion, such a linearization can be justified at intermediate and long distances. It is clear, however, that the linearization strongly diminishes the weight of configurations in which two oppositely charged ions are in a close proximity. Linearization underestimates the strength of electrostatic correlations which result in dipole-like structures. At low reduced temperatures, characteristic of the critical point, these configurations should be quite important and must be taken into account. One way of doing this, while preserving the linearity of the theory, is to postulate the existence of dipoles with concentration governed by the law of mass action. In the leading-order approximation the dipoles can be treated as an ideal non-interacting specie[56, 57, 58]. The total number of particles $N = \rho V$ is then subdivided into monopoles $N_1 = \rho_1 V$ and dipoles $N_2 = \rho_2 V$. The particle conservation requires that, $N = N_1 + 2N_2$. The free energy of the mixture is $F = F_1^{ent} + F_2^{ent} + F^{el}$, where F^{el} and F_1^{ent} are the entropic and the electrostatic free energies of the monopoles, given by Eqs. (13) and (15), but with $N \rightarrow N_1$ and $\rho \rightarrow \rho_1$. The entropic free energy of dipoles is,

$$\beta F_2^{ent} = N_2 \ln[\rho_2 \Lambda^6 / \zeta_2] - N_2, \quad (24)$$

where the internal partition function of a dipole is,

$$\zeta_2(R) = 4\pi \int_a^R r^2 dr \exp\left(\frac{\beta q^2}{\epsilon r}\right). \quad (25)$$

At low temperatures the precise value of the cutoff R at which two ions can be considered to be associated is not very important. Following the original suggestion of Bjerrum[56]

we can take this value to be the inflection point of the integral in Eq. (25), $R_{Bj} = \lambda_B/2$. This choice corresponds to the minimum of integrand in Eq. (25), which in turn can be interpreted as the probability of finding two oppositely charged ions at separation r . The minimum then correspond to a liminal between bound and unbound configurations. A much more careful analysis of the dipolar partition function has been carried out by Falkenhagen and Ebeling based on the resummed virial expansion[58]. They found that that the low temperature expansion of the Bjerrum equilibrium constant is identical to the equilibrium constant which can be constructed on the basis of the resummed virial expansion. Since we are interested in the low temperature regime where the critical point is located, the Bjerrum equilibrium constant, $\zeta_2 \equiv \zeta_2(R_{Bj})$, will be sufficient.

It is important to keep in mind that at this level of approximation the electrostatic free energy F_1^{ent} is only a function of the density of free unassociated ions ρ_1 , since the dipoles are treated as an ideal non-interacting specie. The concentration of dipoles is obtained from the law of mass action

$$\mu_2 = \mu_+ + \mu_- , \quad (26)$$

where the chemical potential of a specie s is

$$\mu_s = \partial F / \partial N_s . \quad (27)$$

Substituting the expression for the total free energy into the law of mass action leads to

$$\rho_2 = \frac{1}{4} \rho_1^2 \zeta_2 e^{2\beta\mu^{ex}} , \quad (28)$$

where the excess chemical potential is $\beta\mu^{ex} = \partial f^{el} / \partial \rho_1$. The critical point can be located from the study of the convexity of the total free energy as a function of ion concentration ρ . There is, however, a simpler way[6]. We observe that at Bjerrum level of approximation, dipoles are ideal non-interacting specie. This means that they are only present as spectators and do not interact with the monopoles in any way. This implies that only the monopoles can drive the phase separation. Thus, at the critical point the temperature must still be $T_c^* = 1/16$ and the density of monopoles must still remain $\rho_{1c}^* = 1/64\pi$, as in the case of the pure *DH* theory. The corresponding density of dipoles at criticality is then given by Eq. (28), with $T_c^* = 1/16 = 0.0625$ and $\rho_{1c}^* = 1/64\pi = 0.00497$. We find that at the critical point the density of dipoles is $\rho_{2c}^* \approx 0.02$. In the vicinity of the critical point there are many more dipoles than monopoles, $\rho_{2c}^* / \rho_{1c}^* \approx 4$. Within the Bjerrum approximation the non-linear correlations, in the form of dipoles, do not affect the critical temperature, but strongly modify the critical density, $\rho_c^* = \rho_{1c}^* + 2\rho_{2c}^* = 0.045$. In spite of the crudeness of approximations, the location of the critical point agrees reasonably well with the Monte Carlo simulations [59, 60, 61], $T_c^* = 0.051$ and $\rho_c^* = 0.079$. The coexistence curve, however, is found to have an unrealistic “banana” shape [6]. To correct this deficiency one must go beyond the “ideal” dipole approximation and allow for the dipole-ion interaction[5, 6]. Most of the fundamental physics of electrostatic correlations, however, is already captured at the level of the Bjerrum approximation.

3. Two-dimensional plasma and the Kosterlitz-Thouless transition

A system which over the years has attracted much attention is the two-dimensional plasma of positive and negative ions interacting by a logarithmic potential. The great interest in 2d plasma is due to the fact that various important physical systems can be mapped directly onto it. Examples include superfluid ^4He films, two-dimensional crystalline solids, and XY magnets [62]. Although a continuous symmetry can not be broken in two dimensions [63], if the Hamiltonian of a system is invariant under an Abelian group, a finite temperature phase transition is possible. This transition occurs as a result of unbinding of the topological defects or “charges”. The defect-mediated phase transitions belong to the universality class of the two-dimensional plasma.

Thirty years ago Kosterlitz and Thouless (KT) have presented a renormalization group study of the 2d plasma [64]. They concluded that at sufficiently low temperature, the 2d plasma becomes an insulator. All the positive and negative ions pair-up forming dipoles. The metal-insulator transition was found to be of an infinite order, characterized by essential singularities in the thermodynamic functions. The KT analysis, however, was restricted to the low ionic densities and it is not clear what happens when the concentration of charged particles is increased. It is tempting to apply to the 2d plasmas analysis similar to the one presented earlier for the 3d electrolytes [65].

We shall study a fluid of disks with diameter a and charge $\pm q$. The solvent is a uniform medium of dielectric constant ϵ . The bare interaction potential for two ions (i, j) separated by a distance r is

$$\varphi(r) = -\frac{q_i q_j}{\epsilon} \ln(r/a) . \quad (29)$$

As in the case of 3d electrolyte, the mean-field contribution to the electrostatic free energy is zero, and all the important physics comes from the electrostatic correlations. We shall account separately for the long-ranged and the short-ranged correlations. The short ranged correlations lead to the formation of dipolar pairs of density ρ_2 , while the long ranged correlations produce the screening. As in the case of 3d electrolyte, the total density of hard discs is divided between dipoles and monopoles, so that $\rho = \rho_1 + 2\rho_2$.

To calculate the electrostatic free energy we fix one ion and study the distribution of other particles around it. It is important to recall that the Poisson equation in 2d differs from the one in 3d by the normalization factor[65],

$$\nabla^2 \phi(r) = -\frac{2\pi}{\epsilon} \rho_q(r) , \quad (30)$$

where $\rho_q(r)$ is the local charge density, and the factor of 2π has been replaced the 4π of the 3d Poisson equation. As before, we shall approximate the potential of mean force by the electrostatic potential and then linearize the Boltzmann factor. Linearization is compensated by the allowance for dipolar formation.

The electrostatic potential for distances $r \leq a$ satisfies the Laplace equation $\nabla^2 \phi = 0$, while for $r > a$ the potential satisfies the Helmholtz equation $\nabla^2 \phi = \kappa^2 \phi$,

with

$$\kappa = \sqrt{\frac{2\pi q^2 \rho_1}{k_B T \epsilon}}, \quad (31)$$

This equations can be easily integrated yielding the electrostatic potential,

$$\phi_{<}(r) = -\frac{q}{\epsilon} \ln(r/a) + \frac{q}{\epsilon} \frac{K_0(\kappa a)}{\kappa a K_1(\kappa a)} \quad \text{for } r \leq a, \quad (32)$$

and

$$\phi_{>}(r) = \frac{q}{\epsilon} \frac{K_0(\kappa r)}{\kappa a K_1(\kappa a)} \quad \text{for } r > a, \quad (33)$$

where $K_\nu(x)$ are the modified Bessel functions of order ν . For large distances, the electrostatic potential decays exponentially fast. Just as in three dimensions, the electrostatic interactions are screened inside the two dimensional plasma,

$$\lim_{r \rightarrow \infty} \phi_{>}(r) \approx \frac{q e^{-\kappa r}}{\epsilon \kappa a K_1(\kappa a)} \sqrt{\frac{\pi}{2\kappa r}}. \quad (34)$$

Eq. (32) consists of two terms, the potential produced by the fixed ion and the induced potential due to the ionic atmosphere,

$$\psi = \frac{q}{\epsilon} \frac{K_0(\kappa a)}{\kappa a K_1(\kappa a)}. \quad (35)$$

Given the induced potential, the electrostatic free energy can be obtained using the familiar Debye charging process, Eq. (12). We find the electrostatic free energy density of the 2d plasma to be

$$\beta f^{el} = \frac{1}{2\pi a^2} \ln[\kappa a K_1(\kappa a)]. \quad (36)$$

At the Bjerrum level of approximation, the electrostatic free energy depends only on the density of monopoles. The total free energy density is $f = f_1^{ent} + f_2^{ent} + f^{el}$, where

$$\beta f_1^{ent} = \rho_1 \ln[\rho_1 \Lambda^2/2] - \rho_1 \quad (37)$$

and

$$\beta f_2^{ent} = \rho_2 \ln[\rho_2 \Lambda^4/\zeta_2] - \rho_2. \quad (38)$$

The internal partition function for 2d dipole is

$$\zeta_2(R) = 2\pi \int_a^R r dr \exp \left[-\frac{\beta q^2}{\epsilon} \ln \left(\frac{r}{a} \right) \right]. \quad (39)$$

It is convenient to define the reduced temperature and density as $T^* = k_B T \epsilon / q^2$ and $\rho^* = \rho a^2$. We note that for low temperatures, $T^* < 1/2$, the integral in Eq (39) converges uniformly as $R \rightarrow \infty$. In this regime it is possible, therefore, to define the internal partition function of dipole as

$$\zeta_2 \equiv \zeta_2(\infty) = \frac{2\pi a^2 T^*}{1 - 2T^*}. \quad (40)$$

The thermodynamic equilibrium requires that for fixed volume and number of particles the Helmholtz free energy be minimum. This is equivalent to the law of mass action

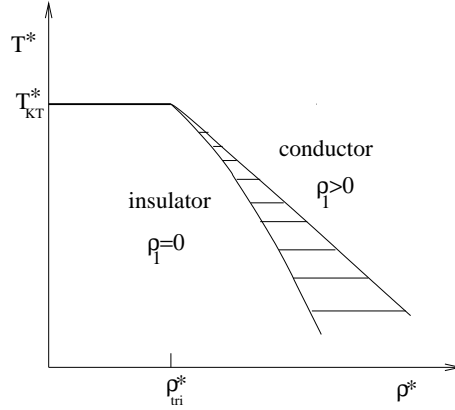


Figure 3. Phase diagram for the two dimensional plasma within the Debye-Hückel-Bjerrum approximation. We expect the fluctuations to renormalize the Kosterlitz-Thouless line, shifting it from its horizontal position and making it density dependent. The topology of the phase diagram should, however, remain the same.

Eq. (26), which upon the substitution of free energy simplifies to Eq. (28). In the limit of small concentrations, the excess chemical potential can be expanded in powers of ρ_1 yielding

$$\beta\mu^{ex} = -\frac{1}{2T^*}[\gamma_E + \ln(\kappa a/2)] , \quad (41)$$

where γ_E is the Euler constant. Substituting Eq. (41) into Eq. (28), we find that the concentration of dipoles in the limit $\rho \rightarrow 0$ scales as

$$\rho_2 \sim \rho_1^{\theta(T^*)} , \quad (42)$$

where

$$\theta(T^*) = 2 - \frac{1}{2T^*} . \quad (43)$$

For $T^* < 1/4$, the exponent $\theta(T^*) < 0$, and in the limit $\rho_1 \rightarrow 0$ the law of mass action can no longer be satisfied. This means that in the temperature density plane (T^*, ρ^*) , for sufficiently small densities, the line $T^* = 1/4$ corresponds to the critical locus of metal-insulator transitions. Below this line, and for sufficiently small ionic concentrations, no free monopoles can exist. All the ions are paired up into neutral dipolar pairs. The critical line terminates at the tricritical point located at $T_{KT}^* = 1/4$ and

$$\rho_{tri}^* = \frac{e^{-4\gamma_E}}{8\pi} \simeq 0.003954 . \quad (44)$$

For $T^* < 1/4$ and $\rho^* > \rho_{tri}^*$ there is a phase separation between an insulating vapor and a conducting liquid phases, Fig 3. As the critical line is approached from high temperatures, the Debye length diverges as

$$\xi_D \equiv \kappa^{-1} \sim e^{c(\rho)/t^\nu} , \quad (45)$$

where

$$c(\rho) = \frac{1}{4} \ln \left(\frac{\rho_{tri}}{\rho} \right) , \quad (46)$$

and

$$t = \frac{T - T_{KT}}{T}, \quad (47)$$

and the critical exponent is $\nu = 1$. The Kosterlitz-Thouless (KT) renormalization group theory [64] predict a similar behavior for ξ_D except that $\nu = 1/2$. The *KT* theory, however, leaves unanswered the question of what happens to the metal-insulator transition for higher plasma concentrations. The current theory, on the other hand, shows that the critical line terminates in a tricritical point, after which the metal-insulator transition becomes first order [65]. This topology is also consistent with the findings of Monte Carlo simulations [66, 67]. A more sophisticated theory introduced by Minhagen [68], leads to a very similar phase diagram, except that the tricritical point is replaced by a critical end-point.

We see that the electrostatic correlations are even more important in 2d than in 3d. While in three dimensions an electrolyte phase separates into coexisting liquid and gas phases, both of which contain monopoles and dipoles, in two dimensions the low density vapor phase does not contain any free charges and is an insulator.

4. The one component plasma

The one component plasma (*OCP*) is probably the simplest model of a Coulomb system. It consists of point ions, all of the same sign, inside a rigid neutralizing background of opposite charge. In spite of its simplicity the model is relevant for many physical systems. Some examples are the interiors of stars, liquid metals, and magnetically confined electrons. As an approximation, *OCP* is particularly important since it provides a framework in which ionic correlations can be calculated. Thus, the electrostatic free energy of a homogeneous *OCP* can be used to account for the counterion correlations in colloidal suspensions and polyelectrolyte solutions. The *OCP* has been extensively studied over the years. A review of the subject, which still remains very actual, has been presented by Baus and Hansen some twenty years ago [69].

In the spirit of the current work we shall, however, confine our attention to simple analytical theories of the *OCP* [70, 71]. Our model consists of N ions each carrying charge q inside a uniform neutralizing background of dielectric constant ϵ and volume V . The average ionic density is $\rho = N/V$. The mean electrostatic potential inside the *OCP* is zero and the free energy is, once again, entirely due to positional correlations between the ions. The advantage of working with the *OCP* is that it contains only two independent length scales: the average separation between the particles $d = (4\pi\rho/3)^{-1/3}$ and the Bjerrum length $\lambda_B = q^2/k_B T \epsilon$. There is only one dimensionless parameter on which all the thermodynamic quantities depend, $\Gamma = \lambda_B/d$. This is quite distinct from the electrolytes and two component plasmas, for which besides d and λ_B there is a third length scale — the ionic diameter a — and the thermodynamics is parametrized by two dimensionless quantities T^* and ρ^* . For electrolytes the limit $a \rightarrow 0$ does not exist, since for point particles the free energy can be lowered indefinitely by collapsing the system

into point-like dipolar pairs.

The calculation of free energy of the *OCP* proceeds along the lines of the Debye-Hückel theory. We fix one ion and study the distribution of other ions around it. The electrostatic potential satisfies the Poisson equation, Eq. (2), with the charge density given by

$$\rho_q(r) = q\rho g(r) - q\rho . \quad (48)$$

The correlation function can be expressed in terms of the potential of mean force $w(r)$ as

$$g(r) = e^{-\beta w(r)} . \quad (49)$$

In the spirit of the Debye-Hückel theory we replace $w(r)$ by $q\phi(r)$. This approximation entails neglect of electrostatic correlations inside the ionic cloud which surrounds the central ion. The approximation should be quite good as long as Γ is not too large. As the next step, linearization of the Boltzmann factor leads to the charge density of particularly simple form,

$$\rho_q(r) = -\frac{\epsilon\kappa^2}{4\pi}\phi(r) , \quad (50)$$

where $\kappa^2 = 4\pi\beta q^2\rho/\epsilon$. Substituting this into the Poisson equation we, once again, find the familiar Helmholtz equation (7). This can be easily integrated yielding the electrostatic potential of Yukawa form,

$$\phi(r) = \frac{qe^{-\kappa r}}{\epsilon r} . \quad (51)$$

The charge density must be bounded from below $\rho_q \geq -q\rho$. However, considering Eqs. (50) and (51), it is evident that this condition is violated for sufficiently small separations from the central ion. Something must have gone seriously wrong. It is easy to trace the problem to the linearization of the Boltzmann factor. Clearly at short distances linearization is not justified since the strong electrostatic repulsion between the ions results in a very large electrostatic energy. It appears that in order to understand the physics of the *OCP* one has to solve the full non-linear Poisson-Boltzmann equation, a task which cannot be performed analytically. Fortunately not everything is lost. A way out was suggested by Nordholm, who noted that the strong repulsion between like charged ions results in an effective hole surrounding the central ion [70]. Very few ions can penetrate inside the hole since this will cost them too much electrostatic energy. Inside this correlation hole, $r \leq h$, the electrostatic potential satisfies the Poisson equation (2) with a uniform background charge density, $\rho_q \approx -q\rho$. In the outside region, where the electrostatic interaction is much weaker, the linearization of the Boltzmann factor is justified and the potential satisfies the Helmholtz equation. Therefore, for $r > h$ the electrostatic potential still has a Yukawa form, but with an undetermined prefactor,

$$\rho_q(r) = \frac{Ae^{-\kappa r}}{r} . \quad (52)$$

The coefficient A can be obtained from the condition of continuity of $\rho_q(r)$ across $r = h$. We find

$$A = -q\rho h e^{\kappa h} . \quad (53)$$

The charge neutrality requires that

$$q - \frac{4\pi}{3}q\rho h^3 + 4\pi \int_h^\infty r^2 dr \rho_q(r) = 0 . \quad (54)$$

The integral can be performed explicitly and the resulting equation solved to determine the size of the correlation hole

$$h = d[\omega(\Gamma) - 1]/\sqrt{3\Gamma} , \quad (55)$$

where

$$\omega(\Gamma) = [1 + (3\Gamma)^{3/2}]^{1/3} . \quad (56)$$

The size of the correlation hole is a monotonically increasing function of the coupling strength. For high temperatures, small couplings, $h \approx \lambda_B$. This is exactly what one might have expected, since on this length scale the electrostatic repulsion becomes comparable to the thermal energy. When the temperature is lowered the kinetic energy diminishes and the particles are strongly scattered by the electrostatic repulsion, causing increase in the size of the correlation hole. For very low temperatures, large Γ , the size of the correlation hole is equal to the average spacing between the particles, $h \approx d$. This is, once again, the correct limiting behavior since at low temperatures the ions tend to keep as far away as possible from their neighbors. For $r > h$ the electrostatic potential follows directly from Eq. (50),

$$\phi_{>}(r) = \frac{4\pi q\rho h e^{-\kappa(r-h)}}{\epsilon\kappa^2 r} . \quad (57)$$

For $r \leq h$ the Poisson equation with a uniform background charge $\rho_q = -q\rho$ must be solved. The solution is easily found to be

$$\phi_{<}(r) = \frac{q}{\epsilon r} + \frac{2\pi q\rho r^2}{3\epsilon} + \psi . \quad (58)$$

The induced potential ψ can be determined from the condition of continuity of electrostatic potential $\phi_{>}(h) = \phi_{<}(h)$, which yields

$$\psi = -\frac{k_B T}{2q} \{[1 + (3\Gamma)^{3/2}]^{2/3} - 1\} . \quad (59)$$

The Debye charging process Eq. (12), yields the electrostatic free energy per particle

$$\frac{\beta F^{el}}{N} = \frac{1}{4} \left[1 - \omega^2 + \frac{2\pi}{3\sqrt{3}} + \ln \left(\frac{\omega^2 + \omega + 1}{3} \right) - \frac{2}{\sqrt{3}} \tan^{-1} \left(\frac{2\omega + 1}{\sqrt{3}} \right) \right] , \quad (60)$$

where $\omega(\Gamma)$ is given by Eq. (56). In the limit of high temperatures, $\Gamma \rightarrow 0$, Eq.(60) reduces to the Debye limiting law, Eq. (14). Furthermore, the free energy agrees with the Monte Carlo simulations with an error of less than 10% over a wide range of coupling

strengths, $0 < \Gamma < 80$. This suggests that inclusion of the correlation hole into Debye-Hückel theory captures most of the essential physics of the *OCP*.

Some caution must be taken when using *OCP* to model real physical systems. For $\Gamma > 3$, the isothermal compressibility and pressure of the *OCP* become negative [69]. This is a consequence of treating the background as a rigid entity and neglecting its pressure. How this can be corrected, in practice, depends on the kind of problem that one wants to study. If one wants to use the *OCP* to model dense ionized matter, the suitable background is the degenerate electron gas. When the free energy of background is added to the *OCP* the pressure and the compressibility remain non-negative for all Γ . An alternative approach was suggested by Weeks, who defined *OCP* as the classical “dense-point limit” of the two component plasma [72]. In this limit, the background is treated as an infinitely dense cloud of point particles each carrying an infinitesimal charge e , so that $e\rho_{back}$ remains constant. Presence of such background does not affect the electrostatics of the *OCP*, but regularizes its pressure and isothermal compressibility, making them non-negative. An interesting byproduct of this analysis is the conclusion that the freezing of the *OCP* occurs without any change in density, i.e. the volume per particle in the fluid and the solid phases are the same [72]. The freezing transition happens at $\Gamma \approx 180$ and the resulting solid phase has the *BCC* structure [73, 69, 74].

4.1. Confined one component plasma

In 1971 Crandall and Williams suggested that electrons trapped on the surface of liquid helium ^4He can crystallize, forming a two dimensional Wigner crystal [75]. Eight years later this order-disorder transition was observed experimentally by Grimes and Adams [76]. In this system electrons obey classical mechanics since the Fermi energy is much smaller than $k_B T$. Similar crystallization can occur in the inversion layer near the surface of a semiconductor, however, in this case the quantum effects are important and the electrons form a degenerate quantum gas [77].

The trapped electrons above the liquid ^4He can be modeled as a confined quasi-two-dimensional plasma of particles interacting by $1/r$ potential. This model is also appropriate for the study of correlations between the condensed counterions on the surface of colloidal particles.

The average spacing between the confined electrons is $d = (\pi\sigma)^{-1/2}$, where σ is the average surface density, $\sigma = N/A$. The dimensionless quantity parameterizing the strength of electrostatic interactions is $\Gamma = q^2/\epsilon k_B T d$. For an infinitesimally thin layer separating two mediums of dielectric constants ϵ_1 and ϵ_2 , the important parameter is the average dielectric constant $\epsilon = (\epsilon_1 + \epsilon_2)/2$. It has been observed in computer simulations [78] that the 2d *OCP* crystallizes into triangular Wigner crystal for $\Gamma > 130$. This value is also in close agreement with the experiments of Grimes and Adams.

We can gain much insight into thermodynamics of 2d *OCP* using the now familiar Debye-Hückel theory. Our model consists of a plasma of point particles of charge q and of a neutralizing background, confined to the interface located at $z = 0$ between two

dielectric half-spaces. For $z < 0$ the dielectric constant is ϵ_1 and for $z > 0$ the dielectric constant is ϵ_2 . Since the half-spaces do not contain any free charges, the electrostatic potential everywhere satisfies the Laplace equation $\nabla^2\phi = 0$. The electrostatic free energy is obtained by fixing one particle and calculating the induced potential resulting from the redistributions of other ions in the $z = 0$ plane. It is convenient to adopt the cylindrical coordinate system, (ϱ, φ, z) , so that the fixed ion is located at $\varrho = 0, z = 0$. Using the azimuthal symmetry and the fact that the electrostatic potential vanishes at infinity, the solution to Laplace equation can be written as [79]

$$\phi_1(\varrho, z) = \int_0^\infty A_1(k) J_0(k\varrho) e^{kz} dk \quad \text{for } z < 0, \quad (61)$$

and

$$\phi_2(\varrho, z) = \int_0^\infty A_2(k) J_0(k\varrho) e^{-kz} dk \quad \text{for } z > 0, \quad (62)$$

where $J_0(x)$ is the Bessel function of order zero.

The functions $A_1(k)$ and $A_2(k)$ can be determined from the boundary conditions, which are: continuity of the electrostatic potential,

$$\phi_2(\varrho, 0) = \phi_1(\varrho, 0), \quad (63)$$

and discontinuity of the displacement field across the $z = 0$ plane. The discontinuity results from the inhomogeneous distribution of interfacial charge induced by the fixed ion,

$$[\epsilon_2 \mathbf{E}_2(\varrho, z) - \epsilon_1 \mathbf{E}_1(\varrho, z)] \cdot \hat{n} = 4\pi\sigma_q(\varrho). \quad (64)$$

From charge neutrality the *average* interfacial charge is zero so that $\sigma_q(\varrho)$ is the result of ionic correlations,

$$\sigma_q(\varrho) = \frac{q\delta(\varrho)}{2\pi\varrho} - q\sigma + q\sigma e^{-\beta q\phi(\varrho, 0)}. \quad (65)$$

The first term of Eq. (65) is the surface charge density of the fixed ion, the second term is due to the uniform negative background, while the last term is the surface charge density of ions confined to the interface. We have, once again, approximated the potential of mean force by the electrostatic potential. In the spirit of Debye-Hückel theory we shall now linearize the Boltzmann factor. The surface charge density reduces to

$$\sigma_q(\varrho) = \frac{q\delta(\varrho)}{2\pi\varrho} - \frac{\epsilon\phi(\varrho, 0)}{2\pi\lambda_{GC}}, \quad (66)$$

where

$$\lambda_{GC} = \frac{k_B T \epsilon}{2\pi q^2 \sigma} \quad (67)$$

is the Gouy-Chapman length.

The continuity of electrostatic potential requires that $A_1(k) = A_2(k)$. Substituting Eqs.(61) and (62) into Eq.(64) and using Eq.(66), we find the electrostatic potential over the full range $-\infty < z < \infty$ to be

$$\phi(\varrho, z) = \frac{q}{\epsilon} \int_0^\infty \frac{k}{k + \lambda_{GC}^{-1}} J_0(k\varrho) e^{-k|z|} dk. \quad (68)$$

For $z = 0$ the integral can be performed explicitly yielding

$$\phi(\varrho, 0) = \frac{q\tau_0(\varrho/\lambda_{GC})}{\epsilon\varrho}, \quad (69)$$

where the functions $\tau_\nu(x)$ are defined as [80],

$$\tau_\nu(x) = 1 - \frac{\pi x^{1-\nu}}{2} [H_\nu(x) - N_\nu(x)], \quad (70)$$

with $H_\nu(x)$ and $N_\nu(x)$ being the Struve and the Bessel functions of order ν , respectively. For large values of x , $\tau_0 \approx 1/x^2$, so that asymptotically,

$$\phi(\varrho, 0) \approx \frac{q\lambda_{GC}^2}{\epsilon\varrho^3}. \quad (71)$$

We conclude that in the case of a confined plasma there is no exponential screening, instead the electrostatic potential is purely algebraic and has the form of a dipole-dipole interaction [69].

There is a well known argument in the condensed matter physics going back all the way to Bloch [81], Peierls [82] and Landau [83] in 1930's, which states that continuous symmetry can not be broken in two dimensions. This means that there can not exist a true two dimensional crystalline order, since it requires breaking translational symmetry. The argument was made rigorous by Mermin, who proved it for particles interacting by short-ranged potentials [63]. It is quite simple to see how this conclusion arises. Suppose that there is a 2d crystal, one can then calculate the mean-square displacement δ^2 of one particle from its equilibrium position due to thermal fluctuations. It is found that $\delta^2 \sim T \ln L$, where L is the characteristic crystal size. For $L \rightarrow \infty$, the mean square displacement diverges for any finite temperature, implying that in thermodynamic limit a 2d crystal is unstable to thermal fluctuations. Although there is no true long-range order in two dimensions for systems with short range forces, there exists a pseudo-long-range order characterized by the algebraically decaying correlation functions. It is not clear, however, to what extent this applies to 2d *OCP*, whose particles interact by a long-ranged $1/r$ potential. Certainly in this case Mermin's proof is no longer valid. However, since the effective interaction potential inside the 2d *OCP* decays as $1/r^3$ suggests that there should not be any long-range order. Whether there is a true long-range order or pseudo-long-range order for 2d *OCP* remains uncertain. Simulations find that for $\Gamma \approx 130$ there is a crystallization transition. It is, however, difficult to say whether the crystalline state has a true long-range order or a pseudo-long-range order [78]. It is also unclear if the transition is of first order or continuous, belonging to the Kosterlitz-Thouless universality class [64, 62]. Existence of the thermodynamic limit for the confined 2d plasmas can also be attributed to the effective renormalization of the interaction potential from non-integrable $1/r$ to integrable (in two dimensions) $1/r^3$ form.

The Helmholtz free energy of a 2d plasma can be obtained directly from Eq. (69). We need to know the induced potential felt by the central ion due to other particles. In the limit $\varrho \rightarrow 0$, the electrostatic potential reduces to

$$\phi(\varrho) \approx \frac{q}{\epsilon\varrho} + \frac{q}{\epsilon\lambda_{GC}} \ln(\varrho/2\lambda_{GC}). \quad (72)$$

The first term of this expression is the potential produced by the central ion, while the second term is the induced potential felt by the fixed ion. We note that the induced potential is actually divergent in the limit $\varrho \rightarrow 0$. This is a consequence of failure of linearization of the Poisson-Boltzmann equation. This deficiency can be corrected in the same way as was done for the 3d *OCP*, by introducing a correlation hole of radius h around each particle. Unfortunately in the present geometry this leads to calculations which are no longer tractable analytically. From our study of the 3d *OCP* we can, however, make some reasonable approximations. In the limit of high temperatures, small Γ , the size of the correlation hole should be such that the electrostatic and the thermal energies become approximately equal,

$$\frac{q^2}{\epsilon h} \approx k_B T. \quad (73)$$

This means that $h \approx \lambda_B$. We can use this value as the short-distance cutoff in the calculation of free energy. The induced potential is then

$$\psi \approx \frac{q}{\epsilon \lambda_{GC}} \ln(\lambda_B / 2 \lambda_{GC}). \quad (74)$$

The free energy is obtained through the usual Debye charging process, Eq. (12). Recalling that $\lambda_B(\lambda q) = \lambda^2 \lambda_B(q)$ and $\lambda_{GC}(\lambda q) = \lambda_{GC}(q) / \lambda^2$, where λ is the charging parameter. In the limit of high temperatures $\Gamma \rightarrow 0$, the reduced free energy per particle is found to be

$$\frac{\beta F^{el}}{N} \approx \Gamma^2 \ln(\Gamma). \quad (75)$$

Eq. (75) is precisely the leading order term of the resumed virial expansion obtained by Totsuji [84, 85].

For low temperatures, the *OCP* crystallizes into triangular lattice. The Madelung energy of this lattice is,

$$\frac{\beta U}{N} = -1.106103 \Gamma. \quad (76)$$

This equation provides a surprisingly good fit not only for the free energy of solid, but also for the free energy of fluid at sufficiently high values of Γ . Comparing to the results of Monte Carlo simulations[78] we find that for $\Gamma = 5$ the error accrued from using Eq. (76) to calculate the total electrostatic free energy is about 30%. For $\Gamma = 20$ this error drops to 11% and for $\Gamma = 50$ it goes down to 6%. Recalling that the crystallization transition occurs at $\Gamma \approx 130$, we see that the Eq. (76) works well into the fluid phase. It is reasonable, therefore, to approximate the free energy of fluid for $\Gamma > 5$ by

$$\frac{\beta F^{el}}{N} = -1.106103 \Gamma. \quad (77)$$

The reason why the electrostatic free energy of the fluid is so well approximated by the free energy of the crystal, is the consequence of strong electrostatic correlations.

5. Asymmetric systems

Up to now we have considered only symmetric plasmas and electrolytes. In practice, however, it is unlikely that both cations and anions have exactly the same size and magnitude of charge. It is, therefore, important to explore the thermodynamics of a general $Z : 1$ electrolyte in which cations have charge Zq and diameter a_c , while anions have charge $-q$ and diameter a_a . Unfortunately, as soon as the asymmetry is introduced, the internal inconsistency enters into the Poisson-Boltzmann equation [49]. Recall that the cation-anion correlation function can be expressed in terms of the potential of mean force w_{+-}

$$g_{+-}(r) = e^{-\beta w_{+-}(r)} . \quad (78)$$

The $w_{+-}(r)$ is the work needed to bring cation and anion from infinity to separation r inside the electrolyte. Clearly this work is invariant under the permutation of particle labels $w_{+-}(r) = w_{-+}(r)$. This means that

$$g_{+-}(r) = g_{-+}(r) . \quad (79)$$

The Poisson-Boltzmann equation, which serves as the basis, for the Debye-Huckel theory, approximates the potential of mean force by $w_{+-}(r) = q_- \phi_+(r)$. The self consistency condition, Eq. (79), then requires that

$$q_+ \phi_-(r) = q_- \phi_+(r) . \quad (80)$$

Because of the non-linear nature of the *PB* equation this condition can not be satisfied except for the symmetric electrolytes. The linearization prescription intrinsic to the Debye-Hückel theory allows Eq. (80) to hold for ions of different valence, but with the *same* ionic diameter, $a_c = a_a$.

We see that as soon as the symmetry between the cations and anions is broken the physics and the mathematics of the problem becomes significantly more complex. In the limit of very large asymmetries, $Z \rightarrow \infty$ and $a_c \gg a_a$ a new simplification, however, enters into the game.

5.1. Colloidal suspensions

A typical colloidal suspension often studied experimentally consists of polystyrene sulphonate spheres of diameter $10\text{nm} - 1\mu\text{m}$ and $10^3 - 10^4$ ionizable surface groups. Because of the large surface charge, the colloidal particles tend to repel each other, forming crystals, even at fairly low volume fraction of less than 10%. Using the periodic structure of the lattice, the thermodynamics of a colloidal crystal can be studied fairly straightforwardly. Each colloidal particle can be thought to be confined to a Wigner-Seitz (WS) polyhedral cell. A further approximation replaces the polyhedral *WS* cell by a sphere [22].

5.2. Colloidal lattices

We shall model the colloidal particles as hard spheres of radius a carrying Z ionizable groups of charge $-q$ distributed uniformly on the surface. The counterions will be idealized as point particles of charge $+q$. The suspension of $N_p = \rho_p V$ polyions and $N_c = ZN_p = \rho_c V$ counterions is confined to the volume V . As usual, the solvent will be treated as a uniform continuum of dielectric constant ϵ . For sufficiently large polyion concentrations colloidal suspension crystallizes. Using the lattice symmetry, we restrict our attention to *one* colloidal particle and its counterions inside a spherical WS cell of radius R such that

$$\rho_p = \frac{1}{\frac{4\pi}{3}R^3} . \quad (81)$$

Using the statistical mechanics it is possible to show that the osmotic pressure inside the cell is proportional to the concentration of counterions at the cell boundary [86],

$$\beta P = \rho_c(R) . \quad (82)$$

The thermodynamics of a crystalline colloidal suspension now reduces to the calculation of the distribution of counterions inside the WS cell. This can be done using a simple mean-field picture. The electrostatic potential inside the WS cell satisfies the Poisson equation (2) with the counterion charge density approximated by the normalized spherically symmetric Boltzmann distribution,

$$\rho_q = ZqN_p \frac{e^{-\beta q\phi(r)}}{4\pi \int_a^R r^2 dr e^{-\beta q\phi(r)}} . \quad (83)$$

The non-linear Poisson-Boltzmann equation can be solved numerically to yield the electrostatic potential and the distribution of counterions inside the cell. In practice it is more convenient to work with the electric field

$$\mathbf{E}(\mathbf{r}) = -\nabla\phi(\mathbf{r}) . \quad (84)$$

The Poisson equation can then be rewritten as

$$\nabla \cdot \mathbf{E}(\mathbf{r}) = \frac{4\pi}{\epsilon} [\rho_q(\mathbf{r}) + q_p(\mathbf{r})] , \quad (85)$$

where $q_p(\mathbf{r})$ is the polyion charge density,

$$q_p(\mathbf{r}) = -\frac{Zq}{4\pi a^2} \delta(|\mathbf{r}| - a) . \quad (86)$$

To simplify the calculations we have uniformly smeared the surface of the polyion. Integrating both sides of Eq. (85) and taking advantage of the divergence theorem, the electric field at distance r from the polyion is

$$E(r) = -\frac{1}{\epsilon r^2} [Zq - \alpha(r)] , \quad (87)$$

where

$$\alpha(r) = \int_{|\mathbf{r}'| < r} d^3\mathbf{r}' \rho_q(\mathbf{r}') \quad (88)$$

is the counterion charge inside the sphere of radius r centered on the colloidal particle. Using the gauge in which $\phi(a) = 0$ the electrostatic potential is

$$\phi(r) = - \int_a^r dr E(r) \quad (89)$$

and the Poisson-Boltzmann equation reduces to an integral equation for the electric field. Note that Eq. (87) naturally incorporates the boundary conditions

$$E(a) = -\frac{Zq}{\epsilon a^2} \quad (90)$$

and

$$E(R) = 0 . \quad (91)$$

Eq. (87) can be solved iteratively to yield the counterion density profile from which all other thermodynamic functions are straightforwardly determined.

For aqueous colloidal lattices with monovalent counterions, the Poisson-Boltzmann equation is in excellent agreement with experiments and simulation. The *PB* equation, however, does not account for the correlations between the counterions and breaks down for low dielectric solvents or for aqueous suspensions with multivalent ions. Fortunately, in the case of colloidal lattices, it is fairly straightforward to account for these effects using the density functional theory.

5.3. Density functional theory (DFT) for colloidal lattices

We shall now construct the Helmholtz free energy functional for a Wigner-Seitz cell of a colloidal lattice. The Helmholtz free energy is a functional of the average local counterion density

$$\rho_c(\mathbf{r}) = \left\langle \sum_{i=1}^{N_c} \delta(\mathbf{r} - \mathbf{r}_i) \right\rangle , \quad (92)$$

where the average is over all possible particle positions. The free energy consists of electrostatic and entropic contributions. The entropic contribution is simply that of an inhomogeneous ideal gas,

$$\beta F^{ent}[\rho_c(\mathbf{r})] = \int d^3\mathbf{r} \rho_c(\mathbf{r}) \{ \ln[\rho_c(\mathbf{r})\Lambda^3] - 1 \} . \quad (93)$$

The electrostatic contribution is the result of Coulomb interactions between the counterions and the polyion, as well as the self-energy of the ionic cloud,

$$F^{el}[\rho_c(\mathbf{r})] = q \int d^3\mathbf{r} d^3\mathbf{r}' \frac{q_p(\mathbf{r}')\rho_c(\mathbf{r})}{\epsilon|\mathbf{r} - \mathbf{r}'|} + \frac{q^2}{2} \int d^3\mathbf{r} d^3\mathbf{r}' \frac{\rho_c(\mathbf{r}')\rho_c(\mathbf{r})}{\epsilon|\mathbf{r} - \mathbf{r}'|} . \quad (94)$$

Eq. (94) is the mean-field approximation for the total electrostatic free energy. It does not account for electrostatic correlations between the counterions surrounding the colloidal particle. Clearly, if there is a counterion present at position \mathbf{r} there is a reduced probability of finding another counterion in its vicinity. This information is not included

in Eq. (94). One can attempt to account for the electrostatic correlations using the local density approximation (*LDA*),

$$\beta F^{cor}[\rho_c(\mathbf{r})] = \int d^3\mathbf{r} \rho_c(\mathbf{r}) f_{cor}[\rho_c(\mathbf{r})] . \quad (95)$$

The correlational free energy can be approximated by the free energy of a three dimensional one component plasma Eq. (60),

$$f_{cor}[\rho_c(\mathbf{r})] \approx f_{ocp}[\rho_c(\mathbf{r})] = \frac{1}{4} \left[1 - \omega^2 + \frac{2\pi}{3\sqrt{3}} + \ln \left(\frac{\omega^2 + \omega + 1}{3} \right) - \frac{2}{\sqrt{3}} \tan^{-1} \left(\frac{2\omega + 1}{\sqrt{3}} \right) \right] , \quad (96)$$

with

$$\omega[\rho_c(\mathbf{r})] = [1 + (3\Gamma[\rho_c(\mathbf{r})])^{3/2}]^{1/3} , \quad (97)$$

where the local coupling strength is,

$$\Gamma[\rho_c(\mathbf{r})] = \lambda_B [4\pi\rho_c(\mathbf{r})/3]^{1/3} . \quad (98)$$

Although Eq. (96) was derived for a plasma in a uniform neutralizing background, it is reasonable to expect that it will also hold for the electrostatic free energy of counterions confined to a *WS* cell. The role of a neutralizing background is played by the confining electric field produced by the colloidal particle.

The equilibrium charge distribution is determined from the minimization of the total Helmholtz free energy

$$F = F^{ent} + F^{el} + F^{cor} \quad (99)$$

subject to the constraint of particle conservation

$$\int d^3\mathbf{r} \rho_c(\mathbf{r}) = N_c . \quad (100)$$

This is equivalent to minimization of the grand potential

$$\Omega = F - \mu_c N_c , \quad (101)$$

where the chemical potential of counterions μ_c is the Lagrange multiplier. Performing the calculation, leads to the equilibrium counterion density profile

$$\rho_c(r) = N_c \frac{e^{-\beta q\phi(r) - \beta\mu^{ex}(r)}}{4\pi \int_a^R r^2 dr e^{-\beta q\phi(r) - \beta\mu^{ex}(r)}} , \quad (102)$$

where the excess chemical potential is,

$$\mu^{ex}(\mathbf{r}) = \frac{\delta F^{cor}}{\delta \rho_c(\mathbf{r})} . \quad (103)$$

We see that in the absence of correlations the density profile reduces to the Boltzmann distribution Eq.(83). The counterion density, which enters into the expression for the excess chemical potential, can be expressed in terms of the electric field,

$$\rho_c(\mathbf{r}) = \frac{\epsilon}{4\pi q} \nabla \cdot \mathbf{E} , \quad (104)$$

which due to spherical symmetry simplifies to

$$\rho_c(r) = \frac{\epsilon}{4\pi q r^2} \frac{\partial(r^2 E)}{\partial r} . \quad (105)$$

Substituting Eq.(102) into Poisson equation (85) and using Eqs. (89) and (105) leads to an integro-differential equation for the electric field, Eq.(87).

Unfortunately, for large colloidal charges this equation has no stable solutions [87, 88, 89]. There is an unbounded increase in the concentration of counterions in the vicinity of the colloidal surface resulting from the failure of the local density approximation. To overcome this difficulty Groot and [89] has suggested use of a weighted density approximation (*WDA*), which has proven quite successful in its application to other problems of condensed matter physics [90, 91]. Within this approach the correlational free energy is given by

$$F^{cor}[\rho_c(\mathbf{r})] = \int d^3\mathbf{r} \rho_c(\mathbf{r}) f_{cor}[\bar{\rho}_c(\mathbf{r})] , \quad (106)$$

where $\bar{\rho}_c(\mathbf{r})$ is the *average* local density,

$$\bar{\rho}_c(\mathbf{r}) = \int d^3\mathbf{r}' w(|\mathbf{r} - \mathbf{r}'|) \rho_c(\mathbf{r}') . \quad (107)$$

The weight function $w(r)$ can be determined from the thermodynamic requirement that

$$\frac{\delta^2 \beta F}{\delta \rho_c(\mathbf{r}) \delta \rho_c(\mathbf{r}')} = \frac{\delta(\mathbf{r} - \mathbf{r}')}{\rho_c(\mathbf{r})} - C_2(|\mathbf{r} - \mathbf{r}'|) , \quad (108)$$

where $C_2(|\mathbf{r} - \mathbf{r}'|)$ is the direct correlation function. In particular this equation must hold in the limit of a homogeneous *OCP*, the direct correlation function for which can be obtained using the theory developed in Section 4 [89],

$$C_2(r) = -\frac{\lambda_B}{h} \quad \text{if } r \leq h , \quad (109)$$

and

$$C_2(r) = -\frac{\lambda_B}{r} \quad \text{if } r > h . \quad (110)$$

Performing the calculation, we find that the weight function is well approximated by [89]

$$w(r) = \frac{3}{2\pi h^2} \left(\frac{1}{r} - \frac{1}{h} \right) \Theta(h - r) , \quad (111)$$

where $\Theta(x)$ is the Heaviside step function, $\Theta(x) = 1$ for $x > 0$ and $\Theta(x) = 0$ for $x < 0$. The *WDA* is significantly more computationally demanding than the *LDA*. Its advantage, however, is the numerical stability for all values of the colloidal charge. The results based on the *WDA* are in excellent agreement with the Monte Carlo simulations. The *WDA* gives us a good handle on thermodynamics of colloidal lattices. At lower concentrations, when the crystalline structure is melted, the situation unfortunately is no longer so clear cut. In this case a simple picture based on the Wigner-Seitz cell is not sufficient and new methods must be developed [23, 92]. Unfortunately the standard techniques of the liquid state theory based on integral equations are powerless in the

case of highly asymmetric colloidal systems. The field theoretic methods also fail when applied to this difficult problem, Fig. 1. Furthermore, even the experimental situation is far from clear. Ise and coworkers claim to have seen stable clusters of colloidal particles in highly deionized colloidal suspensions. Tata *et al.* even report an observation of a full equilibrium vapor-liquid-like phase separation [93]. These experiments, however, have been challenged by Palberg and Würth, who demonstrated that the phase separation observed by Tata *et al.* was the result of non-equilibrium salt gradients produced by the ion exchange resin [94]. In the colloidal science community the possibility of a liquid-vapor phase separation in highly deionized colloidal suspensions has met with large amount of scepticism. The usual argument against the phase transition is based on the Derjaguin-Landau-Verwey-Overbeek (*DLVO*) colloidal pair potential [95, 96].

It is easy to understand the nature of the *DLVO* potential based on the Debye-Hückel theory. If the size of colloidal particles is shrunk to zero, $a \rightarrow 0$, then due to screening by counterions, the interaction energy between two “point” colloids would be of a Yukawa form,

$$V_0(r) = (Zq)^2 \frac{e^{-\kappa r}}{\epsilon r}, \quad (112)$$

where the inverse Debye length is

$$\xi_D^{-1} \equiv \kappa = \sqrt{\frac{4\pi Zq^2 \rho_p}{k_B T \epsilon}}. \quad (113)$$

Now, consider the electrostatic potential outside the fixed colloidal particle of radius a and charge $-Zq$, Eq. (10)

$$\phi_{>}(r) = -\frac{Zq\theta(\kappa a)e^{-\kappa r}}{\epsilon r}, \quad \theta(x) = \frac{e^x}{(1+x)}. \quad (114)$$

Evidently the factor $\theta(\kappa a)$ accounts for the fact that screening starts only outside the cavity, $r > a$. We also can think of Eq. (114) as the potential of a point particle with an effective charge $Q_p = Zq\theta(\kappa a)$. An advantage of this alternative point of view is that the interaction energy for two “point” particles is simply given by Eq. (112) with $Zq \rightarrow Q_p$. This leads directly to the famous *DLVO* potential

$$V_{DLVO}(r) = (Zq)^2 \theta^2(\kappa a) \frac{e^{-\kappa r}}{\epsilon r}. \quad (115)$$

This potential is purely repulsive [97], which naively suggests that a charged colloidal suspension is stable against the liquid-gas phase separation. Sogami and Ise, therefore, have argued that the *DLVO* potential must be incorrect, since it cannot account for the inhomogeneities observed experimentally [98]. In its stead, they proposed a different interaction potential derived on the basis of the Gibbs, instead of the more traditional Helmholtz, free energy. The potential found by Sogami and Ise contains a minimum [98], which implies that at short enough separations the two like-charged colloidal particles attract! What is most surprising is that the attraction appears even for monovalent counterions, i.e in the absence of strong correlations between the colloidal double layers. Furthermore, water is an incompressible fluid so it is difficult to see how a change of

paradigm from Helmholtz to Gibbs free energy can lead to such a profound modification of the interaction potential. Inconsistency in results based on the Helmholtz and the Gibbs free energies has been carefully reexamined by Overbeek, who has traced the discrepancy to a flaw in Sogami and Ise's calculations [99].

It is important to stress that the repulsive two-body interactions do not, in general, preclude the possibility of a liquid-gas phase separation in a multicomponent fluid. In fact van Roij and Hansen found, within the linearized density functional theory, that it is possible for a colloidal suspension with polyions interacting by the repulsive *DLVO* potential to phase separate into coexisting liquid and gas phases [20]. Before entering into the discussion of colloidal fluids it is, however, important to introduce a new fundamental concept — colloidal charge renormalization.

5.4. Charge Renormalization

Although the non-linear Poisson-Boltzmann equation can not be solved analytically for spherical geometry, the numerical solution indicates that the electrostatic potential far from colloidal particle saturates as a function of the bare colloidal charge [22]. This suggests that thermodynamics of a highly charged colloidal systems can be based on the linearized *PB* equation but with a bare colloidal charge replaced by an effective renormalized charge. The original concept of colloidal charge renormalization is due to Alexander et al., but is well predated in the polyelectrolyte literature, where the phenomenon is known as the Manning counterion condensation [100, 101, 102].

To understand better colloidal charge renormalization, let us first consider a uniformly charged plane at fixed potential ψ_s inside a salt solution of concentration c . The electrostatic potential at distance x from the plane satisfies the PB equation,

$$\frac{d^2\phi(x)}{dx^2} = \frac{8\pi c q}{\epsilon} \sinh(\beta q \phi) . \quad (116)$$

Since at the moment we are considering aqueous suspensions containing only monovalent ions, the electrostatic correlations are insignificant and the mean-field Poisson-Boltzmann approximation is sufficient. Multiplying both sides of Eq. (116) by $d\phi/dx$ allows us to perform the first integration. Since the potential vanishes in the limit $x \rightarrow \infty$, we find

$$\frac{1}{2}[\phi'(x)]^2 = \frac{8\pi c}{\epsilon\beta} [\cosh(\beta q \phi) - 1] . \quad (117)$$

The second integration yields [103]

$$\phi(x) = \frac{2k_B T}{q} \ln \frac{1 + e^{-\kappa x} \tanh(\beta q \psi_s/4)}{1 - e^{-\kappa x} \tanh(\beta q \psi_s/4)} , \quad (118)$$

where the inverse Debye length is,

$$\kappa = \sqrt{8\pi c \lambda_B} . \quad (119)$$

In the limit of large surface potentials this expression simplifies to

$$\phi(x) = \frac{2k_B T}{q} \ln \frac{1 + e^{-\kappa x}}{1 - e^{-\kappa x}} . \quad (120)$$

For separations from the plane larger than the Debye length, Eq. (120) becomes

$$\phi(x) = \frac{4k_B T}{q} e^{-\kappa x} . \quad (121)$$

An important observation is that for large surface potentials, $\beta q \psi_s / 4 \gg 1$, the electrostatics away from the plane is completely insensitive to the surface charge density.

Now, let us consider a highly charged colloidal particle of valence Z and radius a inside a symmetric 1 : 1 electrolyte of concentration c . The electrostatic potential at distance r from the center of colloidal particle satisfies the PB equation (6). For distances $r > a + \xi_D$ the electrostatic potential is small and the PB equation can be safely linearized leading to the Helmholtz equation (7). This can be easily integrated yielding the electrostatic potential,

$$\phi(r) = A \frac{e^{-\kappa r}}{r} , \quad (122)$$

where A is an integration constant. To find its value, let's restrict our attention to suspensions in which the $\xi_D \ll a$. In practice this is not a very strong restriction. For salt solutions at physiological concentrations $\xi_D \approx 8 \text{ \AA}$ while the characteristic colloidal size is on the order of 1000 \AA . Even for solutions with very low salt content, in the mM range, the Debye length is on the order of 100 \AA . Under these conditions all the curvature effects associated with the spherical geometry of colloidal particle are effectively screened at separations $a + \xi_D < r < 2a$, and the electrostatic potential is well approximated by that of a uniformly charged plane, Eq. (121). Comparing Eqs. (121) and Eq. (122) the value of the integration constant follows directly, and the electrostatic potential at distance $r > a + \xi_D$ from the center of colloidal particle is

$$\phi(r) = \frac{4k_B T a e^{-\kappa(r-a)}}{q r} . \quad (123)$$

This is the asymptotic solution of the full non-linear PB equation for $\kappa a \gg 1$. Comparing this to the solution of linearized PB , Eq. (114), it is evident that the two are identical as long as *the bare colloidal charge is replaced by the renormalized charge*. For highly charged particles, Eq. (123) shows that the renormalized charge saturates at [104]

$$Z_{ren}^{sat} = \frac{4a(1 + \kappa a)}{\lambda_B} . \quad (124)$$

While the previous analysis was carried out for one colloidal particle inside an electrolyte solution, the concept of charge renormalization is quite general and can be applied to colloidal suspensions under various conditions [105, 105, 106, 107]. The difficulty of defining the effective charge for suspensions at non-zero concentrations resides in the complexity of accounting for the consequences of colloidal interactions. The standard practice is to study one colloidal particle inside a spherical Wigner-Seitz cell whose radius is determined by the volume fraction of colloids [22]. While this procedure is fully justified for colloidal lattices, its foundation is less certain for fluidized suspensions. To find the renormalized charge one numerically solves the full non-linear PB equation

and matches the electrostatic potential to the solution of linearized equation at the cell boundary. Alternatively, the osmotic pressures inside the *WS* cell is calculated using the non-linear and linear equations are matched in order to define the effective charge. One should remember, however, that while at the level of non-linear *PB* equation the osmotic pressure is directly proportional to the concentration of ions at the cell boundary, Eq. (82), this is not the case for the linearized *PB* equation. The various procedures lead to similar values of the renormalized charge. In the case of salt-free suspensions, the effective charge is found to saturate at [22]

$$Z_{ren}^{sat} \approx \frac{15a}{\lambda_B}, \quad (125)$$

and is quite insensitive to the volume fraction of colloidal particles [108, 109].

5.5. Colloidal Fluid

In this section we will apply the insights gained from the study of one and two component plasmas to the exploration of stability of charged colloidal suspensions against the gas-liquid phase separations. We note that the large size asymmetry between colloids and counterions leads to very different equilibration time scales. On the time scale of polyion motion, the counterions are always equilibrated. This suggests that the calculation of free energy should be done in two stages [110]. First, we shall trace out the counterion degrees of freedom, leading to effective many-body interactions between the colloidal particles. Then we will use these effective interactions to calculate the colloid-colloid contribution to the total free energy. The procedure is similar to the one used in McMillan-Mayer theory of solutions [111].

We shall first calculate the contribution to the total free energy arising from the polyion-counterion interactions [23, 92]. Consider suspension in thermal equilibrium. While the colloidal particles are more or less uniformly distributed throughout the solution, the positions of counterions are strongly correlated with the positions of polyions. As a leading order approximation we can, therefore, take the polyion-polyion correlation function to be

$$g_{pp} = 1 \quad (126)$$

and the polyion-counterion correlation function to be

$$g_{pc} = e^{-\beta q \phi(r)}. \quad (127)$$

Choosing the coordinate system in such a way that it is centered on top of one of the colloidal particles, the electrostatic potential at distance $r < a$ satisfies the Laplace equation, while for distances $r > a$ it satisfies the Poisson equation Eq. (2). Based on Eqs. (126) and (127) the charge density in the region $r > a$ can be approximated by,

$$\rho_q(r) = -Zq\rho_p + q\rho_c e^{-\beta q \phi(r)}. \quad (128)$$

In the spirit of the Debye-Hückel theory we shall linearize the exponential [35, 6]. The distribution of charge around the colloid reduces to

$$\rho_q(r) = -\beta q^2 \rho_c \phi(r). \quad (129)$$

For $r > a$ the electrostatic potential, therefore, satisfies the Helmholtz equation (7) with κ given by Eq. (113). The solution to this equation is

$$\phi_{>}(r) = -\frac{Zq\theta(\kappa a)e^{-\kappa r}}{\epsilon r}, \quad (130)$$

while the solution to the Laplace equation for $r \leq a$ is

$$\phi_{<}(r) = -\frac{Zq}{\epsilon a(1 + \kappa a)}. \quad (131)$$

The electrostatic energy due to polyion-counterion interaction is

$$u_p = \frac{1}{2} \int d^3\mathbf{r} [\rho_q(\mathbf{r}) + q_p(\mathbf{r})] \phi(r), \quad (132)$$

where $\rho_q(\mathbf{r})$ is the charge density of counterions given by Eq. (129), and $q_p(\mathbf{r})$ is the charge density of the polyion,

$$q_p(\mathbf{r}) = -\frac{Zq}{4\pi a^2} \delta(|\mathbf{r}| - a). \quad (133)$$

Performing the integration we find

$$u_p = \frac{Z^2 q^2}{2\epsilon(1 + \kappa a)} \left[\frac{1}{a} - \frac{\kappa}{2(1 + \kappa a)} \right]. \quad (134)$$

The electrostatic *free energy* of a polyion inside the suspension is obtained using the Debye charging process [112],

$$\mathcal{F}_p = \int_0^1 d\lambda \frac{2u_p(\lambda q)}{\lambda} = \frac{Z^2 q^2}{2\epsilon a(1 + \kappa a)}. \quad (135)$$

Note that this free energy is the sum of the polyion self energy

$$\mathcal{F}_p^{self} = \frac{Z^2 q^2}{2\epsilon a}, \quad (136)$$

and the solvation energy

$$\mathcal{F}_p^{sol} = -\frac{Z^2 q^2 \kappa a}{2\epsilon a(1 + \kappa a)}, \quad (137)$$

which the polyion gains from being inside the “ionic sea”. The electrostatic free energy due to interaction between all the polyions and counterions is

$$F^{pc} = -\frac{Z^2 q^2 N_p \kappa a}{2\epsilon a(1 + \kappa a)}. \quad (138)$$

We have effectively integrated out the counterion degrees of freedom. This, however, leaves us with the effective many-body potentials of interaction between the colloidal particles. For dilute suspensions, the pairwise interaction potential should be the dominant one. The two-body interaction potential can be obtained from the solution of Helmholtz equation for two colloidal particles [113, 114]. At large separations this leads directly to the *DLVO* interaction potential, Eq. (115). This potential has been extensively tested experimentally and found to work very well for bulk colloidal suspensions [115]. Since the *DLVO* potential is short ranged, the contribution to the total free energy arising from the colloid-colloid interaction can be calculated in the

spirit of the traditional van der Waals theory, through the second virial term. A more sophisticated calculation of the colloid-colloid free energy relies on the Gibbs-Bogoliubov variational bound,

$$F^{pp} \leq F_0 + \langle V_{DLVO} \rangle_0, \quad (139)$$

where the reference system is taken to be the fluid of hard spheres, whose diameter plays the role of a variational parameter. The free energy resulting from the polyion-polyion interaction, F^{pp} , can be approximated by the lowest variational bound of Eq. (139). The calculation is somewhat involved, so we refer the interested reader to the original papers [116, 117, 20, 118].

The entropic mixing free energy of colloids and their counterions is simply that of an ideal gas,

$$\beta F^{ent} = Z N_p [\ln(Z \rho_p \Lambda_c^3) - 1] + N_p [\ln(\rho_p \Lambda_p^3) - 1], \quad (140)$$

where Λ_c and Λ_p are the de Broglie thermal wavelengths of counterions and polyions, respectively.

The total free energy of colloidal suspension is the free energy needed to solvate colloids in the sea of other polyions and counterions $F^{pc} + F^{pp}$, and the free energy of mixing F^{ent} ,

$$F = F^{pc} + F^{pp} + F^{ent}. \quad (141)$$

The osmotic pressure is

$$P = - \left. \frac{\partial F}{\partial V} \right|_{N_p}. \quad (142)$$

It is found that for suspensions with

$$\mathcal{C} \equiv \frac{Z \lambda_B}{a} > 15.2. \quad (143)$$

the pressure is not a convex function of the colloidal concentration, implying existence of a thermodynamic instability. The crucial question is whether this result is reliable? In order to calculate the electrostatic free energies, we were forced to linearize the Boltzmann factor. While this is a reasonable approximation at large separations away from the polyions, linearization is clearly invalid in the vicinity of colloidal surface. There, the strong electrostatic interactions result in accumulation of counterions and the polyion charge renormalization. Therefore, the linear theory can be used *only if* the bare colloidal charge is replaced by the effective renormalized charge, $Z \rightarrow Z_{eff}$, in all the expressions. It was found, however, that the bare charge does not increase without limit but saturates at the value given by the Eq. (125). Substituting $Z \rightarrow Z_{eff}$, into the definition of \mathcal{C} Eq. (143), we see that $\mathcal{C} < 15$, for all values of bare charge Z . The critical threshold, therefore, can not be reached, meaning that a deionized *aqueous* suspensions with *monovalent* counterions is stable against a liquid-gas phase separation for all colloidal charges and sizes [23, 24, 119, 27, 120].

The conclusion that non-linear terms omitted at the level of Debye-Hückel approximation stabilize deionized colloidal suspension against the phase separation has

also been reached by von Grünberg et al. [121, 122, 123] and Tamashiro [124]. Numerical solution of the full non-linear Poisson-Boltzmann equation inside a single Wigner-Seitz cell shows that the osmotic pressure is a monotonically increasing function of colloidal concentration, implying thermodynamic stability at the level of *WS* approximation. Grünberg et al. and Tamashiro, however, demonstrated that the *linearized PB equation* leads to negative compressibility and osmotic pressures for highly charged colloidal particles. This erroneously suggests existence of a thermodynamic instability. Clearly, at the level of the *WS* approximation, the instability is an artifact of linearization. Our calculations suggests that any linear theory, which does not take into account the colloidal charge renormalization, is likely to lead to an erroneous prediction of a liquid-vapor phase separation [20, 125] of a deionized colloidal suspension.

It is curious that the “linear” correlations between colloids and counterions, responsible for the screening of electrostatic interactions, are also the ones driving the suspension towards the phase separation. On the other hand, the “non-linear” correlations responsible for the counterion condensation and charge renormalization, stabilize the suspension against a phase transition.

6. Polyelectrolyte solutions

Polyelectrolytes are polymers with ionizable groups which have tendency to dissociate in polar solvents [126, 127]. The good water solubility of polyelectrolytes is due to large favorable gain in solvation energy resulting from hydration of charged monomers and counterions. Unlike polyampholytes [128, 129, 130, 131], whose monomers can either be cationic (positive) or anionic (negative), all charged monomers of a polyelectrolyte carry charge of the same sign. Depending on the sign of this charge, polyions are either cationic or anionic. Over the last few decades polyelectrolytes have found many industrial applications ranging from water treatment and oil recovery to detergents and superabsorbants. The biological importance of polyelectrolytes, however, has been realized much earlier. After all the most important biomolecule, *DNA*, is an anionic polyelectrolyte [102].

Unlike the simple polymeric fluids, thermodynamics of which is fairly well understood, polyelectrolyte solutions still remain to large extent enigmatic. The difficulty in studying polyelectrolytes resides in the combination of polyion flexibility [132, 133, 134, 126, 135, 136, 137], the long-ranged nature of the Coulomb force, as well as a large charge and size asymmetry between the polyions and the counterions. There are, however, some polyelectrolytes whose polyions are rigid molecules. This allows to bypass the complications associated with the statistics of polyion conformations. We have already come across this kind of systems in our exploration of charged colloidal suspensions. Many biologically relevant polyelectrolytes are also fairly rigid. Persistence length (the distance over which polymer can be considered to be rodlike) for double stranded *DNA* is on the order of 500 Å. Actin filaments, which are the building blocks of a cytoskeleton, have persistence length even

larger, on the order of microns. This should be compared with the Debye length at physiological concentrations of 150 *mM* of *NaCl*, which is about 8 Å. Clearly under these conditions the flexibility of the *DNA* or the actin filaments can be considered an irrelevant perturbation.

The thermodynamics of rodlike polyelectrolytes can be explored using the same theoretical tools used for spherical colloidal suspensions. Rodlike molecules can undergo nematic and smectic phase transitions. For ordered periodic structures, the Wigner-Seitz cell formalism can be employed to obtain most of the relevant thermodynamics [138, 139]. At low volume fraction, when a polyelectrolyte solution is disordered, this strategy is no longer valid and a different methodology must be used. This can be constructed along the same lines taken for colloidal suspensions [140, 141]. The fundamental role of electrostatic correlations between the polyions and counterions appears through the Debye screening of polyion-polyion interactions and renormalization of polyion charge. In polyelectrolyte literature the polyion-counterion association leading to polyion charge renormalization is known as the Manning condensation [100, 102, 101]. Here we will show that Manning condensation is very similar to the charge renormalization found in colloidal suspensions.

First we shall briefly review Manning's original argument [100]. Manning was interested in deriving the limiting (low density) laws for polyelectrolyte solutions, similar to the ones found by Debye and Hückel for simple electrolytes, see Eq. (14). The salient feature of the Debye-Hückel limiting laws is that they do not depend on specifics of electrolyte, i.e. size or hydration. For example, the osmotic pressure at low ionic concentrations is found to be a function only of the ionic charge, temperature, and concentration. The question then arises if such a limiting law is also possible for polyelectrolyte solutions. The answer to this question is far from obvious. The strong electrostatic interaction between the polyions and counterions favors accumulation of counterions in the vicinity of polyions. It is, therefore, possible that even at very large dilutions the physics of a polyelectrolyte solution remains that of a strongly interacting system for which no limiting law should be anticipated [102].

6.1. Manning condensation

Consider a simple model of a polyelectrolyte solution. The rodlike polyions of concentration ρ_p , idealized as rigid cylinders of length L and radius a , carrying Z ionized groups — each of charge $-q$ uniformly spaced along the major axis of the cylinder — inside a uniform dielectric solvent of constant ϵ . The counterions of concentration $\rho_c = Z\rho_p$ will be treated as point particles of charge q . For simplicity we will restrict our attention to the situation in which there is no added salt.

In the low density limit we can neglect the discreteness of polyion charge distribution and assume a uniform line-charge density,

$$\lambda_0 = -\frac{Zq}{L} \equiv -\frac{q}{b}, \quad (144)$$

where b is the separation between the successive charged monomers along the polyelectrolyte chain. The bare interaction potential between a long charged cylinder and a counterion is,

$$\phi = -\frac{2q\lambda_0}{\epsilon} \ln \left(\frac{r}{r_0} \right), \quad (145)$$

where r_0 is the arbitrarily chosen point of zero potential. A polyion-counterion two-body partition function is

$$\zeta_1 = L \int_a^R e^{-\beta q \phi(r)} d^2 r = \pi L r_0 \frac{(R/r_0)^{(2-2\xi)} - (a/r_0)^{(2-2\xi)}}{1 - \xi}, \quad (146)$$

where R is the cutoff distance at which a counterion can still be considered to be bound to the polyion. The Manning parameter is defined as,

$$\xi = \frac{|q\lambda_0|}{\epsilon k_B T} = \frac{q^2}{\epsilon k_B T b}. \quad (147)$$

The integral in Eq. (146) remains finite for all values of ξ . Manning noticed, however, that if the limiting laws exist, thermodynamic functions should be independent of the polyion diameter. However, if $a = 0$ the integral in Eq. (146) diverges as $\xi \rightarrow 1^-$. Manning interpreted this divergence as an indication of counterion condensation. For values of $\xi > 1$ he supposed that n counterions condense onto the polyion, reducing proportionately its effective charge density from λ_0 to

$$\lambda_n = \lambda_0 \frac{Z - n}{Z}. \quad (148)$$

To find the number of condensed counterions n , Manning postulated that for $\xi > 1$ the effective reduced line charge density

$$\xi_{eff} \equiv \frac{|q\lambda_n|}{\epsilon k_B T} \quad (149)$$

saturates at one,

$$\xi_{eff} = 1. \quad (150)$$

If the “renormalized” ξ_{eff} is used in Eq. (146), instead of the “bare” ξ when $\xi > 1$, the polyion-counterion partition function remains finite. Eq. (149) and Eq. (150) determine the number of condensed counterions to be

$$\begin{aligned} n^* &= Z \left(1 - \frac{1}{\xi} \right) \quad \text{for } \xi > 1 \\ n^* &= 0 \quad \text{for } \xi \leq 1 \end{aligned} \quad (151)$$

Once n^* is determined, the rest of the thermodynamic functions can be calculated quite easily. The nice thing about Manning’s argument is that it is so simple. On the other hand it contains some points which might leave a more mathematically inclined reader quite disturbed. Manning relied on existence of the limiting laws to establish the limiting law in the first place! This is a circular logic which is not always guaranteed to work. It is interesting to apply the same argument to the case of a two-dimensional plasma of particles interacting by a logarithmic potential [142], Section 3. Consider

an anion-cation two body partition function Eq. (39). Following Manning, let's look at the limit $a \rightarrow 0$. In this case we find that the integral in Eq. (39) diverges for the temperatures

$$T < T_d \equiv \frac{q^2}{2k_B\epsilon}. \quad (152)$$

Thus, we might incorrectly conclude that the metal-insulator transition also happens at T_d . In reality, we know that the Kosterlitz-Thouless transition occurs at half this temperature,

$$T = T_{KT} \equiv \frac{q^2}{4k_B\epsilon}. \quad (153)$$

For any finite value of the particle diameter, all the thermodynamic functions are analytic at T_d and singularities only appear at $T = T_{KT}$. Therefore, it seems far from obvious if Manning's argument is valid for real polyelectrolytes with monomers and counterions of finite diameter. To explore this in more detail we can appeal to the Debye-Hückel-Bjerrum theory, previously constructed for low dielectric electrolytes, Section 2.2.

6.2. Counterion Association

We will restrict our attention to the salt-free infinite dilution limit. The calculations, however, can be extended to solutions of finite polyelectrolyte concentration as well as to polyelectrolytes with salt or even amphiphiles [141, 143]. As in the case of colloidal fluids, we would like to trace out the degrees of freedom associated with the counterions. This leads to effective many-body interactions between the polyions. In the limit of infinite dilution the contribution from these interactions to the total free energy can be neglected.

Consider a dilute polyelectrolyte solution in thermal equilibrium. If we take a snapshot, we will see polyions distributed more or less uniformly throughout the solution, with no specific orientation. The counterions, on the other hand, will be clustered in the vicinity of polyions. This picture suggests that there are only weak positional correlations between the polyions and strong positional correlations between the polyions and counterions [144]. The average distribution of charge around polyions can, therefore, be approximated by Eq. (128).

Suppose we choose a coordinate system so that it is centered on one of the polyions, with the z -axis along the polyion's major axis. The electrostatic potential for $r < a$ satisfies the Laplace equation, while for $r \geq a$ it satisfies the Poisson equation with the charge distribution approximated by Eq. (128). As in the case of colloids, we would like to linearize the exponential Boltzmann factor. This, however, is prohibited by the fact that electrostatic interactions are very strong in the vicinity of polyion's surface. Thus, in order to linearize the exponential, the short distance polyion-counterion correlations must be explicitly taken into account. In our earlier study of colloidal suspensions this was done by introducing an effective renormalized charge. Here we will take a

somewhat different approach. The main consequence of short distance electrostatic correlations is the polyion-counterion association. This is very similar to the concept of Bjerrum association, which has proven so successful for symmetric 1:1 electrolytes. A polyelectrolyte solution can be thought of as being composed of free unassociated counterions of density ρ_f , as well as of clusters of density ρ_n , consisting of one polyion and some number $0 \leq n \leq Z$ of associated counterions. The polyions with no associated counterions are treated as 0-clusters. The conservation of particles requires that

$$\sum_{n=0}^Z \rho_n = \rho_p . \quad (154)$$

and

$$\rho_f + \sum_{n=0}^Z n \rho_n = Z \rho_p . \quad (155)$$

The distribution of cluster sizes $\{\rho_n\}$ can be determined from the equilibrium condition that the Helmholtz free energy be minimum. Once the clusters are explicitly introduced into the theory, the exponential factor in Eq. (128) can be linearized, since at large distances $\beta q \phi(r) < 1$ and at short distances the “non-linearities” are accounted for through the cluster formation. After linearization, the Poisson-Boltzmann equation reduces to the Helmholtz equation with κ given by,

$$\kappa = \sqrt{\frac{4\pi q^2 \rho_f}{k_B T \epsilon}} . \quad (156)$$

The linear equation can be easily solved yielding the electrostatic potential outside a n -cluster

$$\phi(r) = \frac{2\lambda_n}{\epsilon} \frac{K_0(\kappa r)}{\kappa a K_1(\kappa a)} , \quad (157)$$

where λ_n is the linear cluster charge density of a n -cluster Eq. (148), and $K_\nu(x)$ is the modified Bessel function of order ν . For distances $r < a$ the electrostatic potential is found to be

$$\phi(r) = -\frac{2\lambda_n}{\epsilon} \ln(r/a) + \frac{2\lambda_n}{\epsilon} \frac{K_0(\kappa a)}{\kappa a K_1(\kappa a)} . \quad (158)$$

The electrostatic energy due to n -cluster-counterion interaction can be obtained from Eq. (132) and the electrostatic *free* energy follows from the Debye charging process as in Eq. (135). In the limit of infinite dilution, the electrostatic free energy of a n -cluster is

$$\beta \mathcal{F}_n = -\frac{(Z-n)^2}{Z} \xi \left[\frac{2\gamma_E - 1}{2} + \ln \left(\frac{\kappa a}{2} \right) \right] + \mathcal{O}(\rho_f) . \quad (159)$$

The electrostatic free energy density $f = F/V$ due to all cluster-counterion interactions is

$$\beta f^{pc} = -\frac{\xi}{Z} \sum_{n=0}^Z (Z-n)^2 \rho_n \left[\frac{2\gamma_E - 1}{2} + \ln \left(\frac{\kappa a}{2} \right) + \mathcal{O}(\rho_f) \right] . \quad (160)$$

The cluster-cluster and the counterion-counterion contributions are of higher order in density and in the limit of infinite dilution can be neglected. The only contributions which must still be taken into account are the entropic free energy of mixing and the free energy necessary to construct isolated clusters. Both of which can be concisely written as

$$\beta f^{ent-cl} = \rho_f \ln(\rho_f \Lambda_c^3) + \sum_n \rho_n \ln \left(\frac{\Lambda_n^{3(n+1)} \rho_n}{\zeta_n} \right), \quad (161)$$

where the de Broglie thermal wavelength of a n -clusters is

$$\Lambda_n = \frac{h}{\sqrt{2\pi m_n k_B T}}, \quad (162)$$

and m_n is the cluster geometric mean mass,

$$m_n = (m_p m_c^n)^{\frac{1}{n+1}}. \quad (163)$$

The internal partition function of a n -cluster is

$$\zeta_n = \frac{1}{n!} \int \prod_{i=1}^n \frac{d^3 \mathbf{r}_i}{\Lambda^3} e^{-\beta U}, \quad (164)$$

where U is the usual Coulomb potential. A suitable cutoff must be chosen in order to define what constitutes a cluster. Evaluation of the integral in Eq. (164) represents a formidable task. Fortunately, as we shall see, for polyelectrolyte solutions at infinite dilution specific knowledge of ζ_n proves unnecessary. The total free energy density is then

$$f(\{\rho_n\}) = f^{pc} + f^{ent-cl}. \quad (165)$$

To find the equilibrium cluster distribution, this free energy must be minimized subject to constraints of particle conservation, Eqs. (154) and (155). The minimization is equivalent to the law of mass action,

$$\mu_n = \mu_0 + n\mu_f, \quad (166)$$

where the chemical potential of n -clusters is

$$\mu_n = \frac{\partial f}{\partial \rho_n}, \quad (167)$$

and the chemical potential of free ions is

$$\mu_f = \frac{\partial f}{\partial \rho_f}. \quad (168)$$

Substitution of the total free energy into Eq. (166) leads to the n -cluster distribution

$$\rho_n = \zeta_n \rho_0 \rho_f^n e^{\beta(\mu_0^{ex} + n\mu_f^{ex} - \mu_n^{ex})}, \quad (169)$$

which is actually a set of Z coupled algebraic equations. At large dilutions, the excess chemical potential of n -clusters is

$$\beta \mu_n^{ex} = -\frac{(Z-n)^2}{Z} \xi \left[\frac{2\gamma_E - 1}{2} + \ln \left(\frac{\kappa a}{2} \right) \right] + \mathcal{O}(\rho_f), \quad (170)$$

and of free ions is

$$\beta\mu_f^{ex} = -\xi \sum_{n=0}^Z \frac{(Z-n)^2 \rho_n}{2Z\rho_f} + \mathcal{O}(\rho_f) . \quad (171)$$

The internal partition function of a n -cluster is independent of density. Recalling that $\kappa \sim \sqrt{\rho_f}$, Eq. (169) simplifies to

$$\rho_n \sim \rho_0 \rho_f^{g(n)} , \quad (172)$$

where the exponent is

$$g(n) = \frac{\xi}{2Z} n^2 - \xi n + n , \quad (173)$$

In the limit of infinite dilution, $\rho_f \rightarrow 0$, only the cluster of size

$$n_M = Z \left(1 - \frac{1}{\xi} \right) , \quad (174)$$

which minimizes $g(n)$ survives. In this limit the cluster size distribution takes a particularly simple form,

$$\rho_n = \rho_p \delta_{n, n_M} . \quad (175)$$

This is precisely the cluster size distribution postulated by Manning based on his heuristic argument. The osmotic pressure of a polyelectrolyte solution can be obtained through a Legendre transform of the negative free energy density [142],

$$P = -f(\rho_f, \{\rho_n\}) + \mu_f \rho_f + \sum_n \mu_n \rho_n , \quad (176)$$

which leads directly to the Manning limiting law for pressure [100],

$$\beta P = \left(1 - \frac{1}{2\xi} \right) Z \rho_p \quad for \quad \xi \leq 1 . \quad (177)$$

$$\beta P = \frac{Z \rho_p}{2\xi} \quad for \quad \xi > 1 . \quad (178)$$

The discontinuity in the slope of pressure as a function of temperature has provoked a lot of speculation that the Manning condensation is a real thermodynamic phase transition. Kholodenko and Beyerlein went even so far as to identify Manning condensation with the Kosterlitz-Thouless transition [145]. That this is incorrect follows already from our discussion in Section 6.1. For the two dimensional plasma with logarithmic interactions, the Kosterlitz-Thouless transition occurs at half the equivalent Manning temperature. The two phenomena, therefore, have nothing in common [142]. Furthermore, while the Kosterlitz-Thouless is a real thermodynamic phase transition characterized by the diverging Debye length, for rodlike polyelectrolytes the discontinuity in the slope of pressure appears only in the double limit $\rho_p \rightarrow 0$, $L \rightarrow \infty$. If the order of limits is interchanged, there is no singularity and no counterion condensation. In addition directly at the condensation threshold $\xi = 1$, the Debye length remains finite [141].

For polyelectrolyte solutions containing polyions of *finite* size and at *non-zero* concentration, there is also polyion-counterion association [141]. In this case, however,

the distribution of cluster sizes is no longer a delta-function, but rather a bell-shaped curve centered on some value n^* . We find that n^* depends on the concentration of polyelectrolyte and is somewhat larger than the limiting Manning value n_M . The pressure remains an analytic function of ξ , showing that for real polyelectrolyte solutions, the counterion condensation is actually a crossover phenomenon, very similar to micellar formation in amphiphilic systems [146].

7. Multivalent counterions

Up to now we have been concentrating our attention on aqueous solutions with monovalent counterions. It was already mentioned that in this case the correlations between the condensed counterions can be neglected. To understand why, let us compare the characteristic electrostatic energy of a counterion-counterion interaction to the characteristic thermal energy $k_B T$,

$$\Gamma = \frac{\alpha^2 q^2}{\epsilon d k_B T}, \quad (179)$$

where α is the counterion valence and d is the average separation between the n condensed counterions on the surface of a colloidal particle of radius a . Since $n\pi d^2 = 4\pi a^2$,

$$d = \frac{2a}{\sqrt{n}}, \quad (180)$$

and the coupling strength becomes,

$$\Gamma = \frac{\alpha^2 \lambda_B \sqrt{n}}{2a}. \quad (181)$$

Now, let's consider highly charged latex particles with $Z = 7000$ and $a = 1000 \text{ \AA}$, in water at room temperature. From Eq. (125), $Z_{eff}^{sat} = 2100$, which means that 4900 monovalent ($\alpha = 1$) counterions are condensed onto the particle. The coupling strength of the counterion-counterion interaction is then $\Gamma \approx 0.25$, which clearly shows that the electrostatic interactions between the condensed counterions are very weak. We can make this observation even more general. The highest surface charge concentration σ_m encountered in nature is on the order of one elementary charge per 100 \AA^2 . Let's suppose that suspension consists of highly charged colloidal particles with surface charge density σ_m . Clearly this means that there will be a lot of counterion condensation. For a salt-free colloidal suspension containing multivalent counterions, the number of condensed counterions will be approximately

$$n^* \approx \frac{Z}{\alpha}. \quad (182)$$

The radius of a colloidal particle can be expressed as

$$a = \sqrt{\frac{Z}{4\pi\sigma_m}}. \quad (183)$$

Substituting Eqs. (182) and (183) into Eq. (181) we find that the maximum counterion-counterion coupling strength is,

$$\Gamma_{max} \approx \alpha^{\frac{3}{2}} \lambda_B \sqrt{\pi \sigma_m} . \quad (184)$$

For monovalent counterions $\Gamma_{max} \approx 1.3$, for divalent counterions $\Gamma_{max} \approx 3.6$, and for trivalent counterions $\Gamma_{max} \approx 6.8$. Although Γ_{max} is an overestimate, it clearly shows that for highly charged colloidal particles, correlations between the condensed multivalent counterions cannot be ignored.

7.1. Overcharging

One consequence of strong electrostatic correlations is the phenomenon known as the “overcharging” [147, 148, 149, 150, 151, 152, 153, 154, 155, 156]. Overcharging occurs as the result of highly favorable gain in electrostatic free energy due to strong positional correlations between the condensed counterions.

To understand better how the overcharging of colloidal particles comes about let us consider a simple case of one colloidal particle with a uniform surface charge $-Zq$ and radius a , at zero temperature [157, 158]. The question that we would like to answer is how many α -valent counterions should be placed on top of a colloidal particle in order to minimize the electrostatic energy of the resultant polyion-counterion complex? Naively we might suppose that the number of condensed counterions should be such as to neutralize completely the colloidal charge. This, indeed, would be the case if the charge of counterions was uniformly smeared over the surface of colloid. In reality, the counterions are discrete entities and can gain favorable energy by maximizing their separation from one another. Lets calculate the electrostatic energy of the polyion-counterion complex,

$$E_n = \frac{Z^2 q^2}{2\epsilon a} - \frac{Z\alpha n q^2}{\epsilon a} + F_n^{\alpha\alpha} . \quad (185)$$

The first term is the self energy of a polyion, the second term is the electrostatic energy of interaction between the polyion and n condensed α -ions, and the last term is the electrostatic energy of repulsion between the condensed counterions. Now, consider a one component plasma of n α -ions on the surface of a sphere of radius a but with a *uniform neutralizing background charge* $-\alpha n q$. The electrostatic energy of this *OCP* can be expressed as a sum of contributions arising from the counterion-counterion interaction, counterion-background interaction, and the self energy of the background,

$$F_n^{OCP} = F_n^{\alpha\alpha} - \frac{\alpha^2 n^2 q^2}{\epsilon a} + \frac{\alpha^2 n^2 q^2}{2\epsilon a} . \quad (186)$$

Substituting this expression into Eq. (185), the electrostatic energy of the polyion-counterion complex simplifies to

$$E_n = \frac{(Z - \alpha n)^2 q^2}{2\epsilon a} + F_n^{OCP} . \quad (187)$$

For low temperatures, the condensed counterions try to maximize their separation from one another. In the planar geometry the ground state corresponds to a triangular

Wigner crystal. A similar arrangement of counterions will also be found on the surface of a spherical colloidal particle, up to some topological defects. The electrostatic energy of a planar *OCP* has been discussed in Section 4.1. For a spherical *OCP* the electrostatic energy at zero temperature is

$$F_n^{OCP} = -M \frac{\alpha^2 q^2 n^{3/2}}{2\epsilon a} . \quad (188)$$

where M is the Madelung constant. Because of the topological difference between the plane and the surface of a sphere, we expect that the Madelung constant will not be exactly the same in the two cases. The difference, however, should not be very large as was confirmed in recent Monte Carlo simulations [158]. For concreteness, we shall use $M = 1.106$, the value of the planar *OCP*.

The effective charge of the polyion-counterion complex in units of $-q$ is

$$Z_{eff} = Z - \alpha n^* . \quad (189)$$

where n^* is the number of condensed α -ions which minimize the electrostatic energy,

$$\left. \frac{dE_n}{dn} \right|_{n^*} = 0 . \quad (190)$$

The effective charge is found to be

$$Z_{eff} = -\frac{1 + \sqrt{1 + 4\gamma^2 Z}}{2\gamma^2} , \quad (191)$$

where γ is,

$$\gamma = \frac{4}{3M\sqrt{\alpha}} . \quad (192)$$

We see that the effective charge of a polyion-counterion complex is inverted compared to the bare charge Z of the colloidal particle, so that the complex is overcharged. For highly charged colloids, the effective charge scales as the square root of the bare charge [34, 158],

$$Z_{eff} \approx -\frac{\sqrt{Z}}{\gamma} . \quad (193)$$

The analysis above was conducted for one colloidal particle at zero temperature. For solutions at finite concentration and temperature we face the same difficulties already encountered in our earlier discussion of charge renormalization in colloidal suspensions and polyelectrolyte solutions. In fact the problems are even more severe, since for multivalent counterions the Poisson-Boltzmann equation fails completely. A logical step is to appeal to the density functional theory. The difficulty with the *DFT* lies in constructing a suitable density functional which can take into account the electrostatic correlations. For $Z : \alpha$ suspensions without salt, such functional was presented in Section 5.3. It was found using the *DFT* and the Wigner-Seitz cell formalism [89], that the effective charge Z_{eff} as a function of the bare charge Z , after reaching the maximum decreases, asymptotically going to zero as $Z \rightarrow \infty$. This behavior is in striking contrast to the saturation of the effective charge predicted by the Poisson-Boltzmann theory [22]. Unfortunately it is difficult to construct a suitable density functional for

suspensions containing salt. One alternative is to use the integral equations. The numerical complexity of these theories, however, tends to obscure the essential physics of the problem. Below we shall present a simple phenomenological model of overcharging. Our goal is not the quantitative accuracy, but rather the physical insight into the mechanisms leading to the overcharging in polyelectrolyte solutions.

7.2. Overcharging in electrolyte solutions

Consider a dilute colloidal suspension containing a monovalent salt at concentration c , and α -valent salt at concentration c_α . In aqueous solution the monovalent salt dissociates producing 1 : 1 electrolyte, while the α -valent salt dissociates into α : 1 electrolyte. The inverse Debye length is

$$\xi_D^{-1} = \kappa = \sqrt{8\pi\lambda_B I}, \quad (194)$$

where the ionic strength is

$$I = \frac{1}{2} (\alpha^2 c_\alpha + \alpha c_\alpha + 2c). \quad (195)$$

For simplicity we shall restrict our attention to suspensions with monovalent salt near physiological concentrations — 150mM of *NaCl*. Under these conditions the Debye length is around 8 Å, and the interactions between the colloidal particles can be completely neglected. Furthermore, since the electrostatic attraction between the highly charged α -ions and colloids is so much stronger than the interaction between the monovalent counterions and colloids, the effective charge of a polyion-counterion complex is completely determined by the number of condensed α -ions.

We will define the counterions as free (not-associated) if they are farther than some distance δ from the colloidal surface. The “agglomerate” is then defined as the polyion with the δ -sheath of surrounding counterions. We note, however, that not all of the α -ions which are in agglomerate are actually associated with the polyion. The reason for this is that many of these ions have sufficient kinetic (thermal) energy to leave the vicinity of a colloidal particle. Only the counterions which have the total (kinetic plus potential) energy less than zero can be considered bound to the polyion. Unfortunately, it is not easy to come up with a practical implementation of this energetic criterion, except within a Molecular Dynamics Simulation. On the other hand, a simple geometric criterion based on the polyion-counterion separation is easily implemented. Care, however, must be taken not to count all of the α -ions inside the agglomerate as belonging to the polyion-counterion complex. Below we shall see how this can be accomplished.

We shall take δ to be on the order of few angstroms, corresponding to the radius of a hydrated ion, $\delta \approx 2$ Å. Since the agglomerate is in contact with the bulk, its size is determined by the minimum of the grand potential function

$$\Omega(n) = F(n) - n\mu_\alpha, \quad (196)$$

where $F(n)$ is the Helmholtz free energy of the agglomerate and μ_α is the chemical potential of α -ions inside the sheath. In thermal equilibrium, the chemical potential

of α -ions inside the sheath equals to the chemical potential of α -ions in the bulk of the suspension. At low α -ion concentrations μ_α can be approximated by the chemical potential of an ideal gas,

$$\mu_\alpha = \ln(c_\alpha \Lambda^3) . \quad (197)$$

The Helmholtz free energy of an agglomerate is then

$$F_n = E_n + F_n^{solv} + F_n^{ent} . \quad (198)$$

The electrostatic free energy of an isolated polyion-counterion agglomerate E_n is given by the Eq. (187), the solvation energy that the agglomerate gains when placed in an ionic environment is,

$$F_n^{solv} = -\frac{(Z - \alpha n)^2 q^2 \kappa a}{2\epsilon a(1 + \kappa a)} , \quad (199)$$

see Eq. (137), and the entropic energy of counterions inside the sheath is

$$F_n^{ent} = k_B T [n \ln(\rho_n \Lambda^3) - n] . \quad (200)$$

where,

$$\rho_n = \frac{n}{4\pi a^2 \delta} . \quad (201)$$

For high valence counterions (strong-coupling limit) the free energy of the *OCP* can be approximated by that of a Wigner crystal, see Section 4. If more accuracy is needed, one can use the extrapolation formulas based on Monte Carlo simulations [78]. Here, however, we shall content ourselves with the simplest approximation. The grand potential of an agglomerate is,

$$\beta\Omega(Z, n) = \frac{(Z - \alpha n)^2 \lambda_B}{2a(1 + \kappa a)} - M \frac{\alpha^2 \lambda_B n^{3/2}}{2a} + n \ln(\rho_n / c_\alpha) - n . \quad (202)$$

The number of α -ions n^* inside an agglomerate is determined from the minimum of the grand potential,

$$\left. \frac{\partial \Omega(Z, n)}{\partial n} \right|_{n^*} = 0 . \quad (203)$$

From the previous discussion recall that it is incorrect to associate the effective charge of the polyion-counterion complex with the value of n^* , i.e. $Z_{eff} \neq Z - \alpha n^*$. The reason for this is that not all of the α -ions inside the δ -sheath are actually bound to the polyion. The real number of condensed counterions is $n^* - n_o^*$, where the overestimate n_o^* can be obtained by considering the number of α -ion within a distance δ from the surface of a “neutral” polyion, $Z = 0$

$$\left. \frac{\partial \Omega(0, n)}{\partial n} \right|_{n_o^*} = 0 . \quad (204)$$

The effective charge of a polyion- α -ion complex is then

$$Z_{eff} = Z - \alpha(n^* - n_o^*) . \quad (205)$$

If a small electric field is applied to the suspension, it is the Z_{eff} which will determines the electrophoretic mobility of colloidal particles [156, 106, 159, 107].

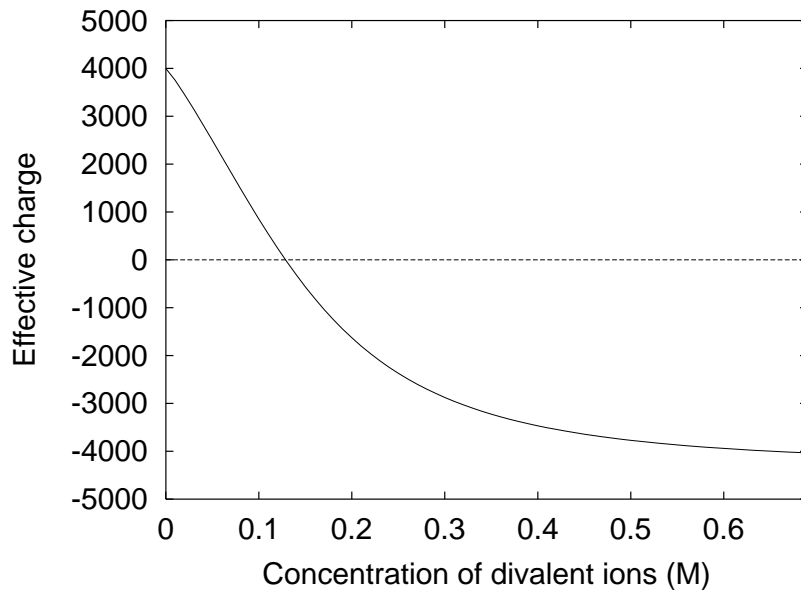


Figure 4. The effective (renormalized) charge of colloidal particles of $Z = 4000$, $a = 1000 \text{ \AA}$ inside a suspension containing monovalent salt at physiological concentration of $0.15M$, as a function of concentration of *divalent* counterions.

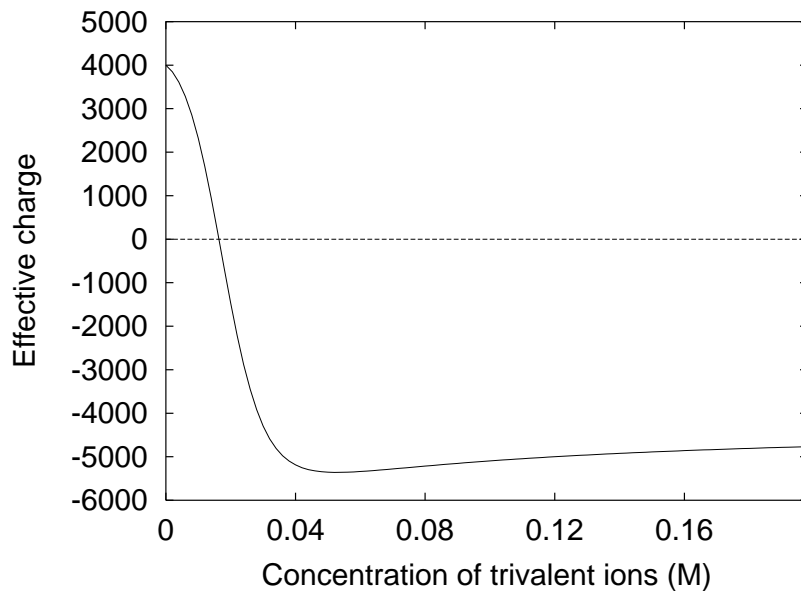


Figure 5. The effective (renormalized) charge of colloidal particles of $Z = 4000$, $a = 1000 \text{ \AA}$ inside a suspension containing monovalent salt at physiological concentration of $0.15M$, as a function of concentration of *trivalent* counterions.

In Figs. 4 and 5 we present the effective colloidal charge as a function of concentration of divalent and trivalent counterions, for suspension containing colloidal particles with $Z = 4000$ and $a = 1000 \text{ \AA}$. It is curious to note the appearance of a minimum in the effective charge as a function of trivalent ion concentration. In Fig. 6

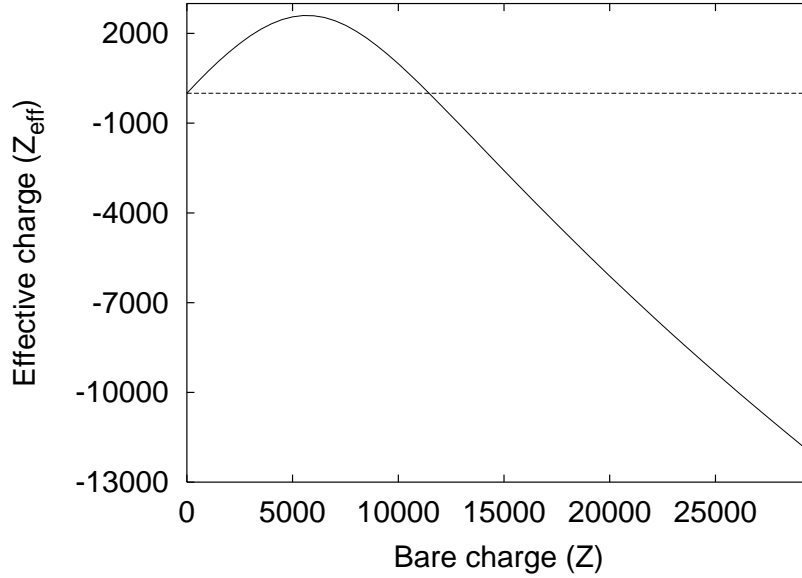


Figure 6. The effective (renormalized) charge of a colloidal particle with $a = 1000 \text{ \AA}$ as a function of the bare charge Z , inside a suspension containing monovalent salt at physiological concentration of $c = 0.15M$ and the trivalent ions at $c_3 = 0.01M$.

we present a plot of the effective charge as a function of bare charge for colloids with $a = 1000 \text{ \AA}$, in a suspension containing monovalent salt at concentration $c = 0.15M$ and trivalent counterions at $c_3 = 0.01M$. We note that unlike suspensions containing monovalent counterions, the effective charge does not saturate, instead it reaches the maximum value and then falls off sharply. For colloids with $Z \approx 11500$, the bare colloidal charge is completely neutralized by the α -ion condensation. In Fig. 7 we show the dependence of Z_{eff} on the amount of monovalent salt. For small concentrations of α -ions, the effective charge of the complex is found to increase with the concentration of monovalent salt, asymptotically approaching the bare value. However, when the concentration of multivalent ions reaches the critical value, there is a qualitative change of behavior. At this point the effective charge is no longer a monotonically increasing function of the monovalent salt concentration. Instead after reaching the maximum, Z_{eff} begins to decline, eventually going through the isoelectric point ($Z_{eff} = 0$) and charge inversion, Fig. 8.

We have considered only the simplest form of overcharging involving colloids and multivalent microions. There is a number of interesting variations. Recent developments in the field of gene therapy require construction of safe and efficient trans-cellular gene delivery systems [160, 161, 162]. Both the DNA and the phospholipids, which are the main constitutive component of a cellular membrane, are negatively charged. There is, therefore, a strong electrostatic repulsion between the DNA and the cellular membrane. This repulsion inhibits the transfection of naked DNA into the cells. Furthermore, *in vivo* the unprotected DNA is rapidly degraded by the nucleases present in plasma [163].

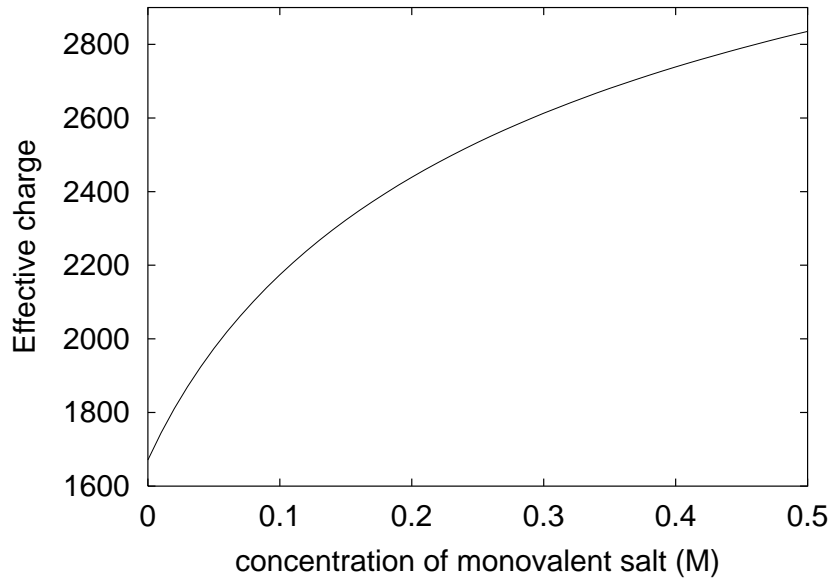


Figure 7. The effective (renormalized) charge of colloidal particles with $Z = 4000$ and $a = 1000 \text{ \AA}$ inside suspension containing trivalent counterions with $c_2 = 0.01M$, as a function of concentration of monovalent salt c .

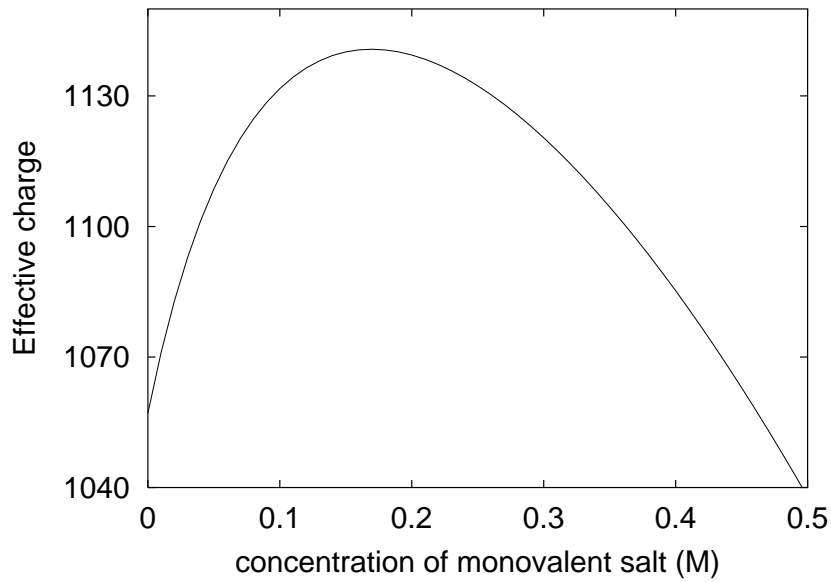


Figure 8. The effective (renormalized) charge of colloidal particles with $Z = 4000$ and $a = 1000 \text{ \AA}$ inside the suspension containing trivalent counterions with $c_2 = 0.0135M$, as a function of concentration of monovalent salt c .

Much of the effort of gene therapy has been concentrated on viral transfection. A retrovirus (virus which incorporates its genetic material into the host genome) or adenovirus (which does not) has its genetic material removed and substituted by the gene that needs to be replicated. The modified virus is then made to infect cells, thus effectuating transfer of genetic material. There are, unfortunately, a number of serious complications involved with this procedure. These range from a strong immunological response of an organism against the infecting virus, to potential deadly consequences arising from the recombinant viral structures [163]. All these factors have lead to attempts to develop non-viral transfection methods. One of the promising approaches relies on formation of the DNA-cationic lipid complexes, or lipoplexes for short. The hydrophobic interactions between the lipid tails, in addition to the cationic charge of their head groups, favors their agglomeration in the vicinity of polyions. For sufficiently long hydrocarbon chains, the gain in hydrophobic energy resulting from the lipid condensation onto the DNA is sufficient to lead to a charge reversal of the lipoplex [164]. This happens even though the charged head group of a lipid is monovalent. The overcharging in this case is the consequence of hydrophobicity of lipid molecules and is not a result of electrostatic correlations.

A different method for gene transfection uses multivalent counterions such as Ca^{++} . The efficiency of Ca^{++} as a transfection agent might be due to its ability to neutralize or even invert the helical DNA charge without making it collapse. In this respect it is quite different from the transition metal ions such as Mn^{++} and Cd^{++} which neutralize the DNA charge, but also lead to its condensation [165]. Formation of a neutral or overcharged DNA- Ca^{++} complex allows the DNA to come into a close proximity of the cellular membrane. Transfection might then be able to proceed through a reptation-like motion of DNA across one of cellular channels.

A very curious form of overcharging is found to occur in cellular compaction of the DNA. Virtually all of the DNA in nuclei of eukaryotic cells exists as a highly organized nucleoprotein fiber called chromatin. At the lowest level of the chromatin hierarchical structure is a nucleosome. Nucleosome resembles a thread wound around a cylindrical spool. The thread is a DNA molecule, while the spool is an octameric protein composed of eight smaller proteins called histones. Each octamer has 220 basic residues of which 148 are on the surface of the protein and are exposed to the solvent [166]. The rest are inside the protein core and are unlikely to be ionised. The maximum charge of an octamer is $Q_{oc}^{max} = +220e$, but is likely to be significantly lower than this value under the normal physiological conditions. Each octamer is encircled by 1.8 turns (147basepairs) of the DNA thread, carrying a net charge of $-294e$. A nucleosome is, therefore, strongly overcharged by the associated DNA [153, 167, 168, 169].

It is interesting to speculate how the nature is using this overcharging in the overall organization of the chromatin. The degree of compaction achieved inside the nucleus is quite astonishing. The total length of the DNA in the nucleus of a human cell is about 3.3 billion base pairs. If extended it would be more than 1m long. Yet, it is compacted into a nucleus of diameter of $10\mu m$! Furthermore, all this compaction is done in such a

way that the DNA is easily transcribed and replicated. This is, indeed, an astonishing feat of chemical engineering!

8. Like-charge attraction

8.1. Confined suspensions

One of the most curious phenomena which has produced much healthy debate in the condensed matter community is the appearance, under some circumstances, of attraction between like-charged macromolecules. The first observation that something might be missing in the traditional *DLVO* theory of colloidal stability came from the experimental observations of Ise et al. of void structures inside the highly deionized suspensions [98]. The finding of voids and clusters has lead Sogami and Ise to propose a modification of the *DLVO* pair potential. In its stead they suggested a new potential obtained from the considerations of the Gibbs free energy of suspension. The Sogami-Ise potential has created a lot of stimulating controversy, which is still in progress. The problem has been re-analyzed by Overbeek [99], who has argued that the Sogami-Ise theory contains a basic thermodynamic inconsistency, which when resolved leads to the usual *DLVO* potential. This, however, has failed to settle the issue and a number of papers are still being published on the thermodynamics of suspensions whose particles interact by the Sogami-Ise potential.

A recently developed Digital Video Microscopy (*DVM*) has the potential of putting an end to this long standing debate. *DVM* provides the possibility of explicitly measuring the interaction potential between two macromolecules in suspension. For dilute bulk suspensions, the interaction potential between two spherical colloidal particles was found to be completely consistent with the *DLVO* theory [115]. A surprising result appeared, however, when a highly deionized suspension is confined between glass plates [115, 170, 171, 172]. It was discovered that when particles are close to a wall, the pairwise interaction potential develops a strong attractive component. The attraction is quite long ranged, comparable in its extent to the diameter of colloidal particle.

It is well known that the glass-water interface has a significant negative charge due to dissociation of silanol groups. This charge density is comparable to that of colloidal particles. Furthermore, the absence of multivalent ions signifies that electrostatic correlations play only a marginal role. Under these conditions the Poisson-Boltzmann theory should work quite well. Indeed, the first numerical solution of the *PB* equation for two macromolecules inside a cylindrical pore has found an attraction between the two polyions [173]. The triumph of the *PB* theory was, however, short lived. Soon afterwards the mathematical proofs were published demonstrating that the *PB* equation is incapable of producing attraction between like-charged particles in confined geometry [174, 175, 176, 177]. The numerical calculation was flawed, a consequence of the intrinsic difficulty of solving numerically non-linear partial differential equations with

complicated boundary conditions. Indeed, it is extremely difficult to understand how a boundary can possibly change the interaction potential from repulsive to attractive. This is not to say that a boundary does not have a profound effect on the interactions. Consider one colloidal particle inside an electrolyte solution at fixed distance from a wall or an interface. In general, the interface is characterized by a dielectric discontinuity. For the moment, however, let's ignore this complication and suppose that the two sides have exactly the same dielectric constant. The interface, then, separates two half-spaces, one containing electrolyte and another electrolyte-free. The fact that all the charges are confined to one half-space strongly modifies the distribution of ions around the colloid. While the ionic cloud is spherically symmetric for colloidal particles far from the interface (in the bulk), it develops a strong asymmetry, which results in a net dipole moment of the colloid-electrolyte system. This dipole produces an electric field,

$$E \sim \frac{1}{r^3} . \quad (206)$$

which, because of the interface, can not be screened. If there are two macromolecules separated by a distance r along the interface, the electric field produced by one macromolecule interacts with the dipole moment \mathbf{p} of the charge distribution induced by the second macromolecule. This leads to the effective interaction potential which is repulsive and falls off as

$$w(r) \approx \mathbf{p} \cdot \mathbf{E} \sim \frac{1}{r^3} , \quad (207)$$

along the direction of an interface [178, 179, 180, 181, 182, 21]. This is exactly the same kind of an effective interaction found for 2d *OCP*, see Section. 4.1.

We see that presence of an interface or a wall strongly modifies the interaction potential between two macromolecules. Instead of an exponential screening found in the bulk, the interactions along an interface falloff algebraically as $1/r^3$. The potential, however, is still repulsive, and it is difficult to see how anything can modify this conclusion at the level of electrostatics.

An interesting suggestion, which seems to account for the apparent attraction between like-charged colloids near a wall, has been recently advanced by Squires and Brenner [183]. These authors attributed the attraction to the non-equilibrium hydrodynamic flows which were not properly accounted for in experiment.

While the hydrodynamics seems to be able to account for the apparent attraction between the colloids near a wall, it is not sufficient to explain the results of experiments in which colloids are sandwiched between two glass plates, since in this geometry the hydrodynamic attraction mediated by one wall is suppressed by the second wall [184]. Furthermore, hydrodynamics does not help to understand the long-lived metastable crystalline structures observed by Grier *et al.* [172, 185] when a low density suspension is compressed against a glass wall. If the interactions between particles are effectively repulsive, once the constraint is removed the crystals should melt within seconds. Instead some crystalline regions are found to survive for as long as an hour. What is even more surprising is that the crystallites are actually three dimensional, extending

far beyond the region where the pairwise surface-mediated attraction is found. This phenomenon is very similar to the voids observed by Ise *et al.*.

The nature of confinement-induced attraction between like-charged particles remains an open question. However, we must stress again that concentrating on pair potentials when studying *thermodynamic stability* of colloidal suspensions is a serious oversimplification. The *DLVO* theory was proposed as an indicator of *dynamical stability* against flocculation, driven by short-ranged van der Waals forces. If the equilibrium structure of a colloidal suspension is in question, interparticle pair potential is not sufficient and the full free energy must be considered. We have already seen in Section 5.5 that a large gain in solvation free energy obtained from the polyion-counterion interaction, strongly favors a phase separation of suspension into coexisting high and low density phases. This tendency is opposed by the counterion condensation, which renormalizes the effective colloidal charge. The theory presented in Section 5.5 suggests that colloidal suspensions should phase separate when $\mathcal{C} > 15.2$. The counterion condensation, however, prevents \mathcal{C} from reaching this threshold. Nevertheless for highly charged colloidal particles, \mathcal{C} can come very close to the critical value, Eq. (125). This suggests that a deionized suspension of highly charged particles might actually be very close to criticality. This regime is characterized by strong density fluctuations, which appear as coexisting domains of voids and crystallites. It is quite possible that this is what has been observed in the experiments of Ise and Grier.

8.2. Correlation-induced attraction

DNA in aqueous solution is highly ionized due to dissociation of phosphate groups. This ionization results in one of the highest charge densities found in nature, one electron charge every 1.7 Å. In spite of this huge charge concentration, over a meter DNA is packed into a nucleus of few micrometers. This efficient compaction is accomplished with the help of cationic proteins. The bacteriophages (viruses that infect bacteria) also use multivalent cations to package their DNA. Thus, the T7 bacteriophage head is 10^{-4} times smaller than the unpacked form of its DNA [186]. Furthermore, it is found that if the multivalent polyamines, known to exist in the host bacteria, are added to an *in vitro* solution containing DNA, the chains condense forming toroids very similar in size and shape to the ones found *in vivo* [29, 30]. To produce condensation, multivalent counterions must somehow induce attraction between the different parts of DNA [187, 188, 189, 190, 191]. The toroidal geometry is a consequence of the high intrinsic rigidity of DNA, which has persistence length of $\xi_p = 500$ Å. If the compaction is done in such a way that the local radius r_c of curvature exceeds $\xi_p/2\pi$ the cost in elastic energy is prohibitively high. Requirement that $r_c > \xi_p/2\pi$, therefore, results in toroidal or spool-like condensates [192, 193].

In eukaryotic cells the cytosol is traversed by a complicated network of microfilaments which are made of a protein called F-actin [32, 194]. In spite of its high negative density charge F-actin, in the presence of multivalent counterions, agglomerates

forming a network of bundles [195]. Addition of monovalent salt screens the electrostatic interactions and re-dissolves the bundles [196]. What is the action of multivalent counterions which induces attraction between the like-charged macromolecules [88, 197, 198, 198, 33, 199, 200, 34, 165, 201, 202, 203, 204, 205, 206, 207, 208]? To understand this we shall look at some very simple models [200].

Consider first two parallel polyions separated by a distance d inside a dilute solution containing α -valent ions. The polyions will be idealized as rigid lines of charge of length $L = Zb$. Each line has Z monomers of charge $-q$ spaced uniformly along the chain. The solvent is a uniform medium of dielectric constant ϵ . It is convenient to define the reduced polyion charge density as $\xi = q^2/\epsilon k_B T b$ [100]. A simple Manning argument then suggests that for $\xi > 1/\alpha$

$$n_c = \frac{Z}{\alpha} \left(1 - \frac{1}{\alpha \xi} \right) \quad (208)$$

α -ions condense onto each polyion. This is the lower bound on condensation, since the Manning argument does not take into account the correlations between the condensed counterions. Nevertheless, even this simple estimate suggest that 88% of the DNA's charge should be neutralized by the divalent counterions.

The associated counterions are free to move along the length of the DNA. We shall suppose that the only effect of condensation is the local renormalization of the monomeric charge from $-q$ to $(-1 + \alpha)q$. Lets define the occupation variables σ_{ij} , with $i = 1, 2, \dots, Z$ and $j = 1, 2$, in such a way that $\sigma_{ij} = 1$, if a counterion is condensed at i 'th monomer of the j 'th polyion, and $\sigma_{ij} = 0$ otherwise. The occupation variables obey the constraint

$$\sum_{i=1}^Z \sigma_{i1} = \sum_{i=1}^Z \sigma_{i2} = n, \quad (209)$$

where n is the number of condensed α -ions. The interaction energy between the two polyions is

$$H = \frac{1}{2\epsilon} \sum_{i,i'=1}^Z \sum_{j,j'=1}^2 \frac{q^2(1 - \alpha\sigma_{ij})(1 - \alpha\sigma_{i'j'})}{r(i, j; i', j')}, \quad (210)$$

where the sum is restricted to $(i, j) \neq (i', j')$, and

$$r(i, j; i', j') = b\sqrt{|i - i'|^2 + (1 - \delta_{jj'})x^2} \quad (211)$$

is the distance between the monomers located at (i, j) and (i', j') . $\delta_{jj'}$ is the Kronecker delta, and $x = d/b$. The partition function is

$$Q = \sum'_{\{\sigma_{ij}\}} \exp(-\beta H), \quad (212)$$

where the prime indicates that the trace is done under the constraint of Eq. (209). The force between the two polyions is

$$F = \frac{1}{b\beta} \frac{\partial \ln Q}{\partial x}. \quad (213)$$

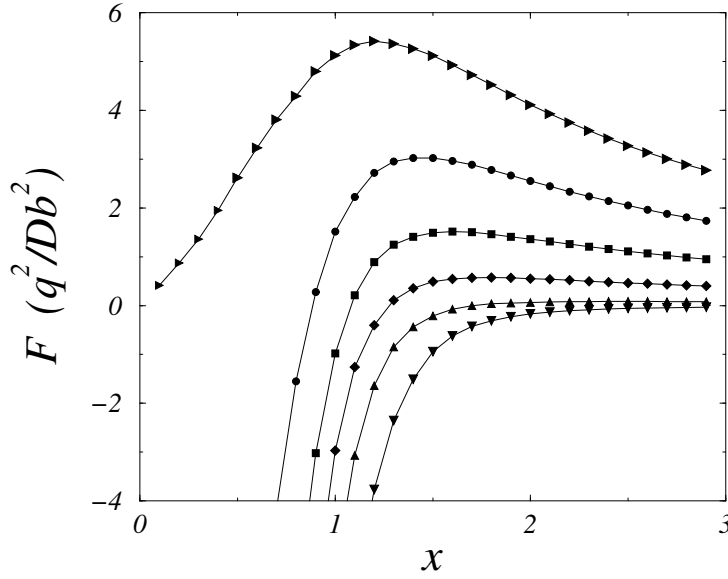


Figure 9. Force versus distance between polyions for $Z = 20$, $\alpha = 2$, $\xi = 2.283$ (corresponding to polymethacrylate) and $n = 5, \dots, 10$ (from top to bottom) in the Monte Carlo simulation [200]. Positive force signifies repulsion between the complexes, while the negative force implies existence of attraction.

This model is so simple that for polyions with not too high values of Z , the partition function can be solved explicitly [200]. For larger Z 's the model can be easily simulated. In Fig. 9 we present the force as a function of separation for two polyions with $Z = 20$ and n condensed divalent counterions. We see that in spite of the net like-charge, the two polyion-counterion complexes can attract each other at sufficiently small separations. Furthermore, we find that a critical number $n_l = Z/2\alpha$ of condensed α -ions is necessary for the attraction to appear and that for monovalent counterions the interaction is always repulsive.

What is the nature of this attraction? To understand this let's consider the limit of small separations between the polyions. The configurations which dominate the partition function for $x \rightarrow 0$ are the ones in which a condensed counterions on one polyion face the bare monomeric charges of the second polyion. The positions of condensed counterions on the two polyions are strongly correlated. The electrostatic energy of such configurations is

$$E \approx \frac{2n(1-\alpha)q^2}{\epsilon bx} + \frac{(Z-2n)q^2}{\epsilon bx}, \quad (214)$$

where n is the number of condensed counterions. The first term of Eq. (214) is the energy due to attractive interaction between n condensed counterions and the bare monomers, while the second term is the repulsive interaction between $Z - 2n$ uncompensated monomeric charges. We see that *if there are $n > Z/2\alpha$ condensed counterions* the first term of Eq. (214) dominates and the force becomes attractive at sufficiently short separations. For $n < Z/2\alpha$ the force is repulsive at any temperature. This is the

general mechanism of attraction between the two polyion-counterion complexes at any finite temperature. To minimize the electrostatic *free* energy, the positions of condensed counterions on the two polyions become correlated. For sufficiently short separations and the number of condensed counterions exceeding the critical threshold n_l , the correlation-induced attraction dominates the monopolar repulsion between the two complexes.

The strength of the counterion correlations increase with the decrease of temperature. The state of maximum correlation is at $T = 0$. This, however, does not imply that the attraction between two polyions is maximum at zero temperature [209]. The reason for this is that the ground state configuration, which corresponds to the lowest electrostatic energy, is not, in general, the configuration which maximizes the attractive force. For low temperatures and short separations there are configurations which have force more attractive than the force in the ground state. For example, consider a polyion with $Z = 6$ and $n = 3$ condensed divalent counterions. The ground state corresponds to a staggered arrangement of counterions on the two polyions. The counterions on one polyion form the pattern $+ - + - + -$ while on the second polyion they form a complimentary pattern $- + - + - +$. This leads to attraction between the complexes. However, it is easy to see that the configuration $+++--$ and $---++$, although it has larger electrostatic energy, leads to stronger attraction. At finite temperature the total force, being a weighted mean of forces associated with all the configurations can, therefore, become more attractive than the force at $T = 0$. This curious behavior, however, is confined to very small separations between the polyions. At larger distances the modulus of the attractive force is a monotonically decreasing function of temperature.

If the number of condensed counterions exceeds

$$n_u = \frac{Z(\alpha + 1)}{2\alpha}, \quad (215)$$

the interaction between the two lines of charge becomes, once again, repulsive. The n_u corresponds to an overcharged configuration in which each polyion has the effective charge

$$Z_{eff}^u = Z - \alpha n_u = -\frac{(\alpha - 1)}{2}Z. \quad (216)$$

It is curious that exactly this kind of reentrant behavior is observed for the DNA condensates [210, 211, 212, 213]. In the absence of multivalent counterions, DNA inside a solution has an extended configuration. When the concentration of multivalent salt is slowly raised, there comes a point at which the gain in electrostatic energy due to polyion- α -ion association overcomes the entropic loss in free energy due to α -ion confinement. The condensed monovalent counterions are then released into solution and are replaced by the polyvalent α -ions. After the critical number of α -ions is associated to the polyion, the interaction between the separate segments of the DNA becomes attractive. This plus the intrinsic rigidity of the molecule drives its condensation into toroidal bundles. As the concentration of multivalent ions in solution is increased further, the DNA- α -ion complex becomes overcharged. When the effective charge of the

polyion reaches Z_{eff}^u , the interaction between the segments of the DNA becomes, once again, repulsive and the bundles re-dissociate. Clearly this simple model is incapable of accounting for all the intricacies of the DNA condensation, nevertheless it sheds a lot of light on the role of electrostatic correlations in this interesting and important phenomenon.

The calculations above were presented for a very idealized model of the interacting lines of charge. It is quite simple to modify the theory to account for a finite polyion diameter. This modification, however, does not significantly affect the predictions of the theory. Attraction appears at small separations between the polyion surfaces — about 7 Å — after the critical number of α -ions is condensed onto the polyions [214]. We find that for macromolecules of finite diameter less counterions are needed to induce attraction than for the two lines of equivalent charge density [214]. Furthermore, the charge-charge correlations along the polyion are of very short range [214, 215], showing absence of any long-range order between the condensed counterions, contrary to the earlier speculations [197, 198, 34].

A very interesting experimental feature of rigid polyelectrolyte solutions containing multivalent counterions is that the correlation-induced attraction does not lead to phase separation [216]. Instead rodlike polyions associate into bundles of well defined thickness. The precise bundle morphology depends on the persistence length of the polyions, all the bundles, however, tend to have a well defined cross-sectional diameter. What can account for this curious phenomenon? Correlation induced attraction should favor an unconstrained growth of bundles [34]. In this respect the situation is very similar to that of an ionic crystal whose electrostatic energy is negative and is unbounded from below. What then cuts off the bundle size? The question is still not fully settled, but the indications are that the size of a bundle is controlled by the kinetics of its formation [217]. To understand this better, let's, once again, consider our simple model of two lines of charge with $n_l < n < Z/\alpha$ condensed α -ions [209]. The polyions are located on two parallel planes separated by a distance d . They are free to rotate in their respective planes. The relative angle between the two lines is θ , with $\theta = 0$ corresponding to two parallel polyions, Fig. 10. It is convenient to define the adimensional free energy as

$$\mathcal{F} = -\frac{1}{\xi} \ln Q , \quad (217)$$

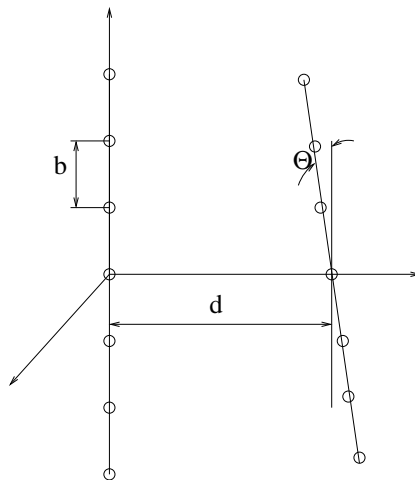


Figure 10. Two rodlike polyions of $Z = 7$.

where Q is the partition function for the two polyions at fixed separation and angular orientation. In Fig. 11 the reduced free energy is plotted as a function of θ for various separations between the polyions. The free energy has two extrema at $\theta = 0$ and $\theta = \pi/2$, corresponding to the parallel and the perpendicular orientation between the polyions. In general, in situations when the attraction appears, the perpendicular configuration has the lowest free energy at large separations between the polyions, while at small distances the parallel configuration minimizes the free energy of the model. However, in some cases, a reentrant behavior is observed. The perpendicular configuration is the global minimum for both large and small distances, while the parallel configuration minimizes the free energy at intermediate distances.

At large separations the like-charged polyion-counterion complexes repel and are perpendicular to one another. When the distance between the polyions is decreased, the global minimum passes from $\theta = \pi/2$ to $\theta = 0$, with $\theta = \pi/2$ becoming metastable. In order for polyions to form a bundle they must align, which means they have to overcome the activation barrier which separates the metastable minimum at $\theta = \pi/2$ from the global minimum at $\theta = 0$. It has been suggested that the height of the barrier that a polyion has to overcome in order to join the already existing bundle, grows with the number of polyions which are already in the bundle [217]. There comes a point when the barrier becomes so high that the thermal fluctuations are unable to overcome it and no new polyion can join the bundle. This puts an end to the bundle growth.

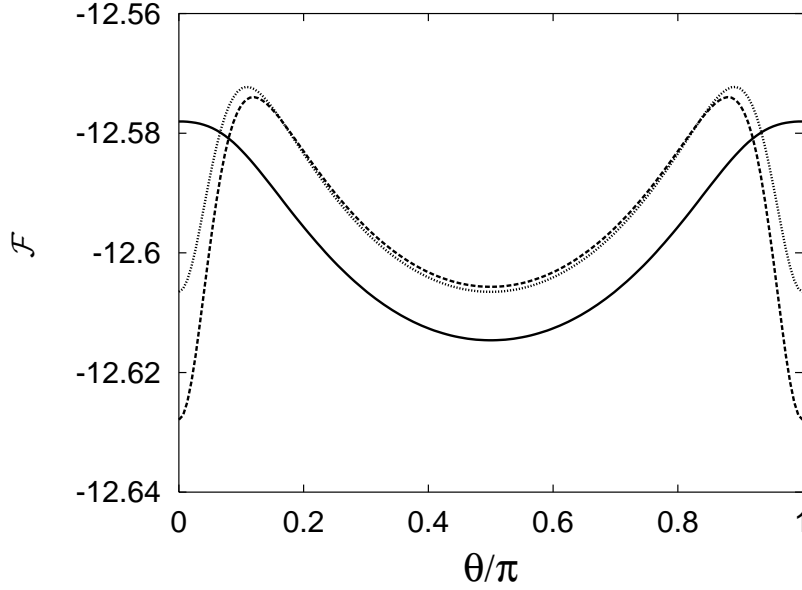


Figure 11. Reduced free energy \mathcal{F} as a function of the angle θ for $Z = 9$, $n = 4$, $\alpha = 2$, $\xi = 2$. The curves shown are for: $x = 2$ (full line), $x = 1.3676$ (dotted line), and $x = 1.3$ (dashed line). Notice that the free energies for $\theta = 0$ and $\theta = \pi/2$ are equal in the second case [209].

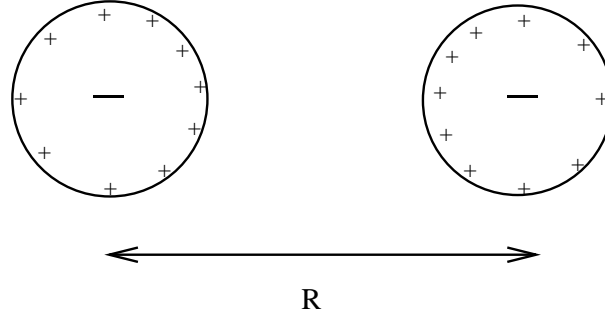


Figure 12. Two polyions with condensed counterions. Note that the net charge Z_{eff} of one complex polarizes the counterions of the other complex.

8.3. Counterion polarization

The correlation-induced attraction between the polyions discussed in the previous section is short ranged, decaying exponentially with the separation between the polyions. The line of charge model is, however, too simple to account for the counterion polarization [218]. Consider for example a rigid cylinder-like polyion or a spherical colloidal particle with a layer of condensed counterions. Suppose that there is no overcharging so that only some fraction of the polyion charge is neutralized by the condensed counterions. The electric field produced by one complex polarizes the counterions of the other complex, Fig. 12. This mechanism certainly provides an attractive component to the interaction potential [219]. However, can this induced

attraction overcome the monopolar repulsion from the uncompensated colloidal charge Z_{eff} ? To understand this let's consider two colloidal particles or globular proteins separated by distance R inside an electrolyte solution with inverse Debye length ξ_D . Each polyion has radius a , charge Z , and n condensed α -ions. The leading order interaction between the two macromolecules at separation $R > \xi_D$ is of *DLVO* form

$$V_{DLVO}(R) = Z_{eff}^2 q^2 \theta^2(\kappa a) \frac{e^{-\kappa R}}{\epsilon R}, \quad (218)$$

where $Z_{eff} = Z - \alpha n$. The major corrections come from two effects. First, presence of polyions produces holes in the ionic atmosphere. The charge of a hole is minus the charge of counterions excluded from the region of space occupied by the macromolecule [113, 114]. For example, the charge of the hole produced by the polyion \mathcal{P}_2 in the ionic atmosphere polarized by the polyion \mathcal{P}_1 is

$$Q_{h,2}(R) \approx -\frac{4\pi a^3 \rho_q(R)}{3}, \quad (219)$$

where the charge density at position R is given by the familiar Debye-Hückel expression,

$$\rho_q(R) = -\frac{\epsilon \kappa^2}{4\pi} \phi(R) = Z_{eff} q \kappa^2 \theta(\kappa a) \frac{e^{-\kappa R}}{4\pi R}. \quad (220)$$

Use of the linearized Debye-Hückel theory is justified by the fact that in Eq. (220) enters the renormalized effective charge. The electrostatic energy of the polyion-hole interaction is obtained using the charging process in which $q \rightarrow \lambda q$ and

$$V_h(R) = Q_{h,2}(R) \int_0^1 d\lambda \phi(R; \lambda q) = \frac{1}{6} \kappa^2 a^3 Z_{eff}^2 q^2 \theta^2(\kappa a) \frac{e^{-2\kappa R}}{\epsilon R^2}, \quad (221)$$

at fixed κ . The second major correction to the DLVO potential is the result of polarization of the condensed layer of counterions surrounding the polyion. Thus, the electric field produced by the complex \mathcal{P}_1 induces a dipole moment in the complex \mathcal{P}_2 , and vice-versa. The local surface charge density of \mathcal{P}_2 is

$$\sigma(\mathbf{r}) = -\sigma_- + \sigma_+ e^{-\beta \alpha q \phi(\mathbf{r})}, \quad (222)$$

where

$$\sigma_- = \frac{Zq}{4\pi a^2}, \quad (223)$$

$$\sigma_+ = \frac{\alpha n q}{4\pi a^2}, \quad (224)$$

and $\phi(\mathbf{r})$ is the local electrostatic potential felt by the condensed counterions at position \mathbf{r} . In the weak coupling limit $\Gamma < 1$ the exponential in Eq. (222) can be linearized yielding the surface charge distribution

$$\sigma(\mathbf{r}) = \Delta\sigma - \frac{\epsilon \phi(\mathbf{r})}{2\pi \lambda_{GC}}, \quad (225)$$

where $\Delta\sigma = \sigma_+ - \sigma_-$ and the Gouy-Chapman length is

$$\lambda_{GC} = \frac{\epsilon}{2\pi \sigma_+ \beta \alpha q}. \quad (226)$$

It is a straightforward calculation in electrostatics to show that the induced dipole moment of the complex \mathcal{P}_2 is

$$\mathbf{p} = \frac{2a^4\epsilon\mathbf{E}}{(3\lambda_{GC} + 2a)}. \quad (227)$$

The electric field produced by \mathcal{P}_1 at distance R from its center is

$$\mathbf{E}(\mathbf{R}) = Z_{\text{eff}}q\theta(\kappa a) \frac{e^{-\kappa R}(1 + \kappa R)\mathbf{R}}{\epsilon R^3}. \quad (228)$$

The electrostatic energy of the induced dipole of \mathcal{P}_2 inside the electric field produced by \mathcal{P}_1 is obtained using the charging process

$$V_p = \int_0^1 d\lambda \mathbf{p}(\lambda q) \cdot \mathbf{E}(\lambda q), \quad (229)$$

where it is important to remember that $\lambda_{GC}(\lambda q) = \lambda^{-2}\lambda_{GC}(q)$. The same argument can be equally well applied to the interaction of \mathcal{P}_2 with the hole produced by \mathcal{P}_1 and to polarization of \mathcal{P}_1 by the electric field produced by \mathcal{P}_2 . Summing up all of these contributions leads to

$$W(R) = Z_{\text{eff}}^2 q^2 \theta^2(\kappa a) \frac{e^{-\kappa R}}{\epsilon R} - Z_{\text{eff}}^2 q^2 \kappa^2 a^3 \theta^2(\kappa a) h\left(\frac{a}{\lambda_{GC}}\right) \frac{e^{-2\kappa R}}{\epsilon R^2}, \quad (230)$$

where the scaling function $h(x)$ is,

$$h(x) = \frac{2}{3} - \frac{3}{2x} \ln\left(1 + \frac{2x}{3}\right). \quad (231)$$

The correction to the *DLVO* potential is repulsive (hole dominated) for $a/\lambda_{GC} < 1.716...$ and is attractive (dipole dominated) for $a/\lambda_{GC} > 1.716...$. We note, however, that it is always “doubly” screened and is, therefore, smaller than the leading order *DLVO* term for separations $R > \xi_D$ [220]. At shorter distances the approximations used to arrive at Eq. (230) fail, and the correlations between the condensed counterions must be explicitly taken into account [16]. For multivalent counterions, the electrostatic correlations result in short-ranged attraction, similar to the one discussed in the previous section.

9. Conclusions

We have explored the role of electrostatic correlations in systems ranging from classical plasmas to molecular biology. We saw how the positional correlations between the ions of electrolyte can lead to phase separation. We also saw how the strong correlations between the polyions and the counterions result in colloidal charge renormalization which stabilizes deionized suspensions against the phase separation. For two-dimensional plasma electrostatic correlations lead to metal-insulator transition. The critical behavior of superfluid ^4He films, the roughening transition of crystal interfaces [221], the melting of two-dimensional solids, and the criticality of XY magnets [62] all are governed by the “electrostatic” interactions between the topological defects (charges). Nature has learned to take the full advantage of electrostatic

correlations to efficiently package huge amounts of genetic material into tiny regions of space.

Throughout this review we have come to rely on some simple models in order to understand complex physical phenomena. While these models are often sufficient to grasp the underlying physics, it is quite easy to push the models too far. This is particularly the case when one deals with specific structural properties of biomolecules [222, 223, 224]. As soon as the length scales on the order of few angstroms become important, approximation of water as a uniform dielectric medium is no longer sufficient [225, 226]. Under these conditions reliance on simple models, which treat macromolecules and solvent as dielectrics, is probably no more than a wishful thinking. A careful path must be threaded between the simplification and over-simplification.

10. Acknowledgements

I am grateful to J.J. Arenzon, M.C. Barbosa, A. Diehl, M.E. Fisher, J.E. Flores-Mena, P. Kuhn, X.-J. Li, J. Stilck, and M.N. Tamashiro who have collaborated closely with me on topics covered in this review. Special thanks are due to Michael Fisher and Shubho Banerjee who have kindly provided me with Fig. 1 which compares the predictions of various theories of asymmetric electrolytes. Last but not least, I would like to thank Eric Westhof without whose encouragement this review would not have been written.

- [1] J. D. van der Waals, Ph.D. thesis, Leiden, 1873.
- [2] P. Weiss, J. Phys. Radium, Paris **6**, 667 (1907).
- [3] G. L. Gouy, J. de Phys. **9**, 457 (1910).
- [4] D. L. Chapman, Phil. Mag. **25**, 475 (1913).
- [5] M. E. Fisher and Y. Levin, Phys. Rev. Lett. **71**, 3826 (1993).
- [6] Y. Levin and M. E. Fisher, Physica A **225**, 164 (1996).
- [7] B. Groh and S. Dietrich, Phys. Rev. E **50**, 3814 (1994).
- [8] B. Groh and S. Dietrich, Phys. Rev. E **54**, 1687 (1996).
- [9] B. Groh and S. Dietrich, Phys. Rev. Lett. **79**, 749 (1997).
- [10] S. Banerjee, R. B. Griffiths, and M. Widom, J. Stat. Phys. **93**, 109 (1998).
- [11] P. G. de Gennes and P. Pincus, Phys. Kondens. Mater. **11**, 189 (1970).
- [12] G. S. Rushbrooke, G. Stell, and J. S. Høye, Molec. Phys. **26**, 1199 (1973).
- [13] J. J. Weis and D. Levesque, Phys. Rev. Lett. **71**, 2729 (1993).
- [14] J.-M. Caillol, J. Chem. Phys. **98**, 9835 (1993).
- [15] M. E. van Leeuwen and B. Smit, Phys. Rev. Lett. **71**, 3991 (1993).
- [16] Y. Levin, Phys. Rev. Lett. **83**, 1159 (1999).
- [17] R. P. Sear, Phys. Rev. Lett. **76**, 2310 (1996).
- [18] R. van Roij, Phys. Rev. Lett. **76**, 3348 (1996).
- [19] J. M. Tavares, M. M. Telo da Gama, and M. A. Osipov, **56**, R6252 (1997).
- [20] R. van Roij and J. P. Hansen, Phys. Rev. Lett. **79**, 3082 (1997).
- [21] J. P. Hansen and H. Löwen, Annual Reviews of Phys. Chem, **51**, 209 (2000).
- [22] S. Alexander *et al.*, J. Chem. Phys. **80**, 5776 (1984).
- [23] Y. Levin, M. C. Barbosa, and M. N. Tamashiro, Europhys. Lett. **41**, 123 (1998).
- [24] A. Diehl, M. C. Barbosa, and Y. Levin, Europhys. Lett. **53**, 86 (2001).
- [25] G. N. Patey, J. Chem. Phys. **72**, 5763 (1980).
- [26] L. Guldbrand, B. Jonsson, H. Wennerstrom, and P. Linse, J. Chem. Phys. **80**, 2221 (1984).
- [27] P. Linse and V. Lobaskin, Phys. Rev. Lett. **83**, 4208 (1999).
- [28] V. Lobaskin, J. Mol. Liq. **84**, 131 (2000).
- [29] V. A. Bloomfield, Biopolymers **31**, 1471 (1991).
- [30] V. A. Bloomfiel, Biopolymer **44**, 269 (1997).
- [31] S. M. Klimenko, J. Mol. Biol. **23**, 523 (1967).
- [32] J. X. Tang, Ber. Bunsenges. Phys. Chem. **100**, 796 (1996).
- [33] B.-Y. Ha and A. J. Liu, Phys. Rev. Lett. **79**, 1289 (1997).
- [34] B. I. Shklovskii, Phys.Rev.Lett. **82**, 3628 (1999).
- [35] P. W. Debye and E. Hückel, Phys. Z. **24**, 185 (1923).
- [36] Netz R. R. and H. Orland, Europhys. Lett. **45**, 726 (1999).
- [37] L. Belloni, Phys. Rev. Lett. **57**, 2026 (1986).
- [38] M. E. Fisher and S. Fishman, Phys. Rev. Lett. **47**, 421 (1981).
- [39] L. Belloni, J. Chem. Phys. **98**, 8080 (1993).
- [40] A. K. Sabir, L. B. Bhuiyan, and C. W. Outhwaite, Mol. Phys. **93**, 405 (1998).
- [41] A. Z. Panagiotopoulos and M. E. Fisher, Phys. Rev. Lett. **88**, 045101 (1992).
- [42] P. J. Camp and G. N. Patey, J. Chem. Phys. **111**, 9000 (1999).
- [43] K.-C. Ng, J. Chem. Phys. **61**, 2680 (1974).
- [44] R. Kjellander and S. Marcelja, Chem. Phys. Lett. **112**, 49 (1984).
- [45] R. Kjellander and S. Marcelja, **90**, 1230 (1986).
- [46] J. P. Hansen and I. R. McDonald, *Theory of Simple Liquids* (Academic Press, NY, 1976).
- [47] S. Arrhenius, Z. Phys. Chem. **1**, 631 (1887).
- [48] S. Glasstone, *Textbook of Physical Chemistry* (D. van Nostrand Company, Inc., NY, 1946).
- [49] L. Onsager, Chem. Revs. **13**, 1933 (1933).
- [50] M. E. Fisher, X.-J. Li, and Y. Levin, **79**, 1 (1995).
- [51] K. S. Pitzer, J. Phys. Chem. **99**, 13070 (1995).

- [52] T. Narayanan and K. S. Pitzer, J. Chem. Phys. **102**, 8118 (1995).
- [53] T. Narayanan and K. S. Pitzer, Phys. Rev. Lett. **73**, 3002 (1994).
- [54] M. E. Fisher and B. P. Lee, Phys. Rev. Lett. **77**, 3561 (1996).
- [55] E. Luijten, M. E. Fisher, and A. Z. Panagiotopoulos, cond-mat/0112388 (unpublished).
- [56] N. Bjerrum, Kgl. Dan. Vidensk. Selsk. Mat.-fys. Medd. **7**, 1 (1926).
- [57] W. Ebeling, Z. Phys. Chem.(Leipzig) **238**, 400 (1968).
- [58] H. Falkenhagen and W. Ebeling, in *Ionic Interactions*, edited by S. Petrucci (Academic Press, NY, 1971).
- [59] J. M. Caillol, D. Leveuque, and J. J. Weis, J. Chem. Phys. **107**, 1565 (1997).
- [60] G. Orkoulas and A. Z. Panagiotopoulos, J. Chem. Phys. **110**, 1581 (1999).
- [61] Q. Yan and J. J. de Pablo, J.Chem.Phys. **111**, 9509 (1999).
- [62] D. Nelson, in *Phase Transitions and Critical Phenomena*, edited by C. Domb and J. L. Lebowitz (Academic Press, NY, 1983), p. 1.
- [63] N. D. Mermin, Phys. Rev. **171**, 272 (1968).
- [64] J. Kosterlitz and D. Thouless, J. Phys. C **6**, 1181 (1973).
- [65] Y. Levin, X.-J. Li, and M. E. Fisher, Phys. Rev. Lett. **73**, 2716 (1994).
- [66] J.-M. Caillol, J. Chem. Phys. **100**, 2161 (1994).
- [67] G. Orkoulas and A. Z. Panagiotopoulos, J. Chem. Phys. **104**, 7205 (1996).
- [68] P. Minnhagen, Rev. Mod. Phys. **59**, 1001 (1987).
- [69] M. Baus and J. P. Hansen, Physics Reports **59**, 1 (1980).
- [70] S. Nordholm, Chem. Phys. Lett. **105**, 302 (1984).
- [71] M. N. Tamashiro, Y. Levin, and M. C. Barbosa, Physica A **268**, 24 (1999).
- [72] J. D. Weeks, Phys. Rev. B **24**, 1530 (1981).
- [73] E. L. Pollock and J. P. Hansen, Phys. Rev. A **8**, 3110 (1973).
- [74] F. J. Rogers, D. A. Young, H. E. DeWitt, and M. Ross, Phys. Rev. A **28**, 2990 (1983).
- [75] R. S. Crandall and R. Williams, Phys. Lett. A **34**, 404 (1971).
- [76] C. C. Grimes and G. Adams, Phys. Rev. Lett. **42**, 795 (1979).
- [77] A. V. Chaplik, Sov. Phys. JETP **35**, 395 (1971).
- [78] R. C. Gann, S. Chakravarty, and G. V. Chester, Phys. Rev. B **20**, 326 (1979).
- [79] J. E. Flores-Mena, M. C. Barbosa, and Y. Levin, Phys. Rev. E **63**, 066104 (2001).
- [80] E. S. Velazquez and L. Blum, Physica A **244**, 453 (1997).
- [81] F. Bloch, Z. Phys. **61**, 206 (1930).
- [82] R. E. Peierls, Ann. Inst. Henri Poincare **5**, 177 (1935).
- [83] L. D. Landau, Phys. Z. Sowjetunion **II**, 26 (1937).
- [84] H. Totsuji, J. Phys. Soc. Jpn. **39**, 253 (1975).
- [85] H. Totsuji, J. Phys. Soc. Jpn. **40**, 857 (1976).
- [86] H. Wennerström, B. Jönsson, and P. Linse, J. Chem. Phys. **76**, 4665 (1982).
- [87] R. Penfold, S. Nordholm, B. Jönsson, and C. E. Woodward, J. Chem. Phys. **92**, 1915 (1990).
- [88] M. J. Stevens and M. O. Robbins, Europhys. Lett. **12**, 81 (1990).
- [89] R. D. Groot, J. Chem. Phys. **95**, 9191 (1991).
- [90] P. Tarazona, Phys. Rev. A **31**, 2672 (1985).
- [91] W. A. Curtin and N. W. Ashcroft, Phys. Rev. A **32**, 2909 (1985).
- [92] M. N. Tamashiro, Y. Levin, and M. C. Barbosa, Physica A **258**, 341 (1998).
- [93] B. V. R. Tata, M. Rajalakshmi, and A. Arora, Phys. Rev. Lett. **69**, 3778 (1992).
- [94] T. Palberg and M. Wurth, Phys. Rev. Lett. **72**, 786 (1994).
- [95] B. V. Derjaguin and L. Landau, Acta Physicochimica (USSR) **14**, 1941 .
- [96] E. J. W. Verwey and J. T. G. Overbeek, *Theory of the Stability of Lyophobic Colloids* (Elsevier, Amsterdam, 1948).
- [97] M. O. Robbins, K. Kremer, and G. S. Grest, J. Chem. Phys. **88**, 3286 (1988).
- [98] I. Sogami and N. Ise, J. Chem. Phys. **81**, 6320 (1984).
- [99] J. T. G. Overbeek, J. Chem. Phys. **87**, 4406 (1987).

- [100] G. S. Manning, J. Chem. Phys. **51**, 924 (1969).
- [101] F. Oosawa, *Polyelectrolytes* (Marcel Dekker, NY, 1971).
- [102] G. S. Manning, Q. Rev. Biophys. II **2**, 179 (1978).
- [103] W. B. Russel, D. A. Saville, and W. R. Schowalter, in *Colloidal Dispersions*, edited by G. K. Batchelor (Cambridge University Press, Cambridge, 1989).
- [104] E. Trizac, L. Bocquet, and M. Aubouy, cond-mat/0201510 (unpublished).
- [105] M. Quesada-Pérez, J. Callejas-Fernández, and R. Hidalgo-Álvarez, Phys. Rev. E **61**, 574 (2000).
- [106] A. Fernández-Nieves, A. Fernández-Barbero, and F. J. de las Nieves, Langmuir **16**, 4090 (2000).
- [107] A. Fernandez-Nieves, A. Fernandez-Barbero, and F. J. de las Nieves, Phys. Rev. E **63**, 041404 (2001).
- [108] M. J. Stevens, M. L. Falk, and M. O. Robbins, J.Chem.Phys. **104**, 5209 (1995).
- [109] L. Belloni, Colloids and Surfaces A **140**, 227 (1998).
- [110] H. Löwen, J. P. Hansen, and P. A. Madden, J. Chem. Phys. **98**, 3275 (1993).
- [111] W. G. McMillan and J. E. Mayer, J. Chem. Phys. **13**, 276 (1945).
- [112] R. A. Marcus, Free energy and pressure in PB equation **23**, 1057 (1955).
- [113] X.-J. Li, Y. Levin, and M. E. Fisher, Europhys. Lett. **26**, 683 (1994).
- [114] M. E. Fisher, Y. Levin, and X.-J. Li, J. Chem. Phys. **101**, 2273 (1994).
- [115] J. M. Crocker and D. G. Grier, Phys. Rev. Lett. **73**, 352 (1994).
- [116] G. A. Mansoori and F. B. Canfield, J. Chem. Phys. **51**, 4958 (1969).
- [117] B. Firey and N. W. Ashcroft, Phys. Rev. A **15**, 2072 (1977).
- [118] P. B. Warren, J. Chem. Phys. **112**, 4683 (2000).
- [119] P. Linse and V. Lobaskin, J. Chem. Phys. **112**, 3917 (2000).
- [120] P. Linse, J. Chem. Phys. **113**, 4359 (2000).
- [121] H. H. von Grünberg, R. van Roij, and G. Klein, Europhys. Lett. **55**, 580 (2001).
- [122] M. Deserno and H. H. Grünberg, cond-mat/0202029 (unpublished).
- [123] R. Klein and H. H. von Grünberg, Pure Appl. Chem. **73**, 1705 (2001).
- [124] M. N. Tamashiro (unpublished).
- [125] D. Y. C. Chan, P. Linse, and S. N. Petris, Langmuir **17**, 4202 (2001).
- [126] J.-L. Barrat and J.-F. Joanny, Advances in Chemical Physics **94**, 1 (1996).
- [127] R. Netz and D. Andelman, cond-mat/0203364 (unpublished).
- [128] P. G. Higgs and J.-F. Joanny, J. Chem. Phys. **94**, 1543 (1991).
- [129] Y. Kantor and M. Kardar, Phys. Rev. E **51**, 1299 (1995).
- [130] A. V. Dobrynin and M. Rubinstein, J. Phys. II (France) **5**, 677 (1995).
- [131] Y. Levin and M. C. Barbosa, Europhys. Lett. **31**, 513 (1996).
- [132] P. G. de Gennes, P. Pincus, and R. M. Velasco, J. Phys. (France) **37**, 1461 (1976).
- [133] A. R. Khokhlov, J. Phys. A **13**, 979 (1980).
- [134] M. J. Stevens and K. Kremer, J. Chem. Phys. **103**, 1669 (1995).
- [135] A. V. Dobrynin, M. Rubinstein, and S. P. Obukhov, Macromolecules **9**, 2974 (1996).
- [136] U. Micka, C. Holm, and K. Kremer, Langmuir **15**, 4033 (1999).
- [137] N. Lee and D. Thirumalai, Macromolecules **34**, 3446 (2001).
- [138] R. M. Fuoss, A. Katchalsky, and Lifson S., Proc. Natl. Acad. Sci. USA **37**, 579 (1951).
- [139] M. Deserno and C. Holm, in *Electrostatic Effects in Soft Matter and Biophysics*, edited by C. Holm and et al. (Kluwer, Dordrecht, 2001), Vol. 46.
- [140] Y. Levin, Europhys. Lett. **34**, 405 (1996).
- [141] P. Kuhn, Y. Levin, and M. C. Barbosa, Macromolecules **31**, 8347 (1998).
- [142] Y. Levin, Physica A **257**, 408 (1998).
- [143] P. Kuhn, Y. Levin, and M. C. Barbosa, Chem. Phys. Lett. **298**, 5 (1998).
- [144] H. Löwen, J. Chem. Phys. **100**, 6738 (1994).
- [145] A. L. Kholodenko and A. L. Beyerlein, Phys. Rev. Lett. **74**, 4679 (1995).
- [146] J. N. Israelachvili, D. J. Mitchell, and B. W. Ninham, J. Chem. Society-Faraday Trans. II **72**, 1525 (1976).

- [147] G. M. Torrie and J. P. Valleau, *J. Chem. Phys.* **73**, 5807 (1980).
- [148] E. Gonzales-Tovar, M. Lozada-Cassou, and D. Henderson, *J. Chem. Phys.* **83**, 361 (1985).
- [149] M. Lozada-Cassou, R. Saavedra-Barrera, and D. Henderson, *J. Chem. Phys.* **77**, 5150 (1982).
- [150] R. Messina, E. G. Tovar, M. Lozada-Cassou, and C. Holm, cond-mat/0111335 (unpublished).
- [151] T. T. Nguyen and B. I. Shklovskii, cond-mat/0005304 (unpublished).
- [152] T. T. Nguyen, A. Y. Grosberg, and B. I. Shklovskii, *Phys. Rev. Lett.* **85**, 1568 (2000).
- [153] A. Y. Grosberg, T. T. Nguyen, and B. I. Shklovskii, *Reviews of Modern Physics*, **74**, 329 (2002).
- [154] T. T. Nguyen, A. Y. Grosberg, and B. I. Shklovskii, *Phys. Rev. Lett.* **85**, 1568 (2000).
- [155] T. T. Nguyen, A. Y. Grosberg, and B. I. Shklovskii, *J. Chem. Phys.* **113**, 1110 (2000).
- [156] M. Tanaka and A. Y. Grosberg, *J. Chem. Phys.* **115**, 567 (2001).
- [157] R. Messina, C. Holm, and K. Kremer, *Phys. Rev. Lett.* **85**, 872 (2000).
- [158] R. Messina, C. Holm, and K. Kremer, *Phys. Rev. E* **64**, 021405 (2001).
- [159] R. Golestanian, *Europhys. Lett.* **52**, 47 (2000).
- [160] T. Friedmann, *Sci. Am.* **276**, 80 (1997).
- [161] P. L. Felgner, *Sci. Am.* **276**, 86 (1987).
- [162] P. L. Felgner and G. M. Ringold, *Nature* **337**, 387 (1989).
- [163] M. J. Hope, B. Mui, S. Ansell, and Q. F. Ahkong, *Mol. Membrane Biol.* **15**, 1 (1998).
- [164] P. S. Kuhn, Y. Levin, and M. C. Barbosa, *Physica A* **274**, 8 (1999).
- [165] A. A. Kornyshev and S. Leikin, *Phys. Rev. Lett.* **82**, 4138 (1999).
- [166] S. N. Khrapunov, A. I. Dragan, A. V. Sivolob, and A. M. Zagariya, *Biochimica et Biophysica Acta-Gene Structure and Expression* **1351**, 213 (1997).
- [167] D. Andelman and J.-F. Joanny, *Cr. Acad. Sci. IV-Phys.* **1**, 1153 (2000).
- [168] S. Y. Park, R. F. Bruinsma, and W. M. Gelbart, *Europhys. Lett.* **46**, 493 (1999).
- [169] E. M. Mateescu, C. Jeppesen, and P. Pincus, *Europhys. Lett.* **46**, 493 (1999).
- [170] G. M. Kepler and S. Fraden, *Phys. Rev. Lett.* **73**, 356 (1994).
- [171] D. G. Grier and J. C. Crocker, *Phys. Rev. E* **61**, 980 (2000).
- [172] D. G. Grier, *J. Phys.:Cond. Mat.* **12**, A85 (2000).
- [173] W. R. Bowen and A. O. Sharif, *Nature* **393**, 663 (1998).
- [174] J. Neu, *Phys. Rev. Lett.* **82**, 1072 (1999).
- [175] J. Sader and D. Y. C. Chan, *J. Colloid Interfacial Sci.* **213**, 268 (1999).
- [176] E. Trizac, *Phys. Rev. E* **62**, R1465 (2000).
- [177] E. Trizac and J. L. Raimbault, *Phys. Rev. E* **60**, 6530 (1999).
- [178] B. Jancovici, *J. Stat. Phys.* **28**, 43 (1982).
- [179] B. Jancovici, *J. Stat. Phys.* **29**, 263 (1982).
- [180] D. Goulding and J. P. Hansen, *Mol. Phys.* **95**, 649 (1998).
- [181] D. Goulding and J. P. Hansen, *Europhys. Lett.* **46**, 407 (1999).
- [182] R. Allen, J. P. Hansen, and S. Melchionna, **3**, 4177 (2001).
- [183] T. Squires and M. Brenner, *Phys. Rev. Lett.* **86**, 5266 (2001).
- [184] D. G. Grier, private communication (unpublished).
- [185] A. E. Larsen and D. G. Grier, *Phys. Rev. Lett.* **76**, 3862 (1996).
- [186] L. C. Gosule and J. A. Schellman, *Nature* **259**, 333 (1976).
- [187] H. H. Strey, R. Podgornik, D. C. Rau, and V. A. Parsegian, *Cur. Opin. in Structural Biology* **8**, 309 (1998).
- [188] R. Podgornik and V. A. Parsegian, *Phys. Rev. Lett.* **80**, 1560 (1998).
- [189] R. Golestanian, M. Kardar, and T. B. Liverpool, *Phys. Rev. Lett.* 4456 (1999).
- [190] F. Solis and M. de la Cruz, *J. Chem. Phys.* **112**, 2030 (2000).
- [191] G. Ariel and D. Andelman, cond-mat/0206361 (unpublished).
- [192] T. Odijk, *Biophys. J.* **75**, 1223 (1998).
- [193] S. Y. Park, D. Harries, and W. M. Gelbart, *Biophys. J.* **75**, 714 (1998).
- [194] J. X. Tang and P. A. Janmey, *J. Biol. Chem.* **271**, 8556 (1996).
- [195] I. Borukhov, R. F. Bruinsma, W. M. Gelbart, and A. J. Liu, *J. Chem. Phys.* **117**, 462 (2002).

- [196] J. X. Tang, P. T. Szymanski, P. A. Janmey, and T. Tao, *Eur. J. Biochem.* **247**, 432 (1997).
- [197] I. Rouzina and V. Bloomfield, *J. Chem. Phys.* **100**, 9977 (1996).
- [198] N. Grønbech-Jensen, R. J. Mashl, R. F. Bruinsma, and W. M. Gelbart, *Phys. Rev. Lett.* **78**, 2477 (1997).
- [199] Y. Levin, J. J. Arenzon, and J. F. Stilck, *Phys. Rev. Lett.* **83**, 2680 (1999).
- [200] J. J. Arenzon, J. F. Stilck, and Y. Levin, *Eur. Phys. J. B* **12**, 79 (1999).
- [201] A. A. Kornyshev and S. Leikin, *Phys. Rev. E* **62**, 2576 (2000).
- [202] E. Allahyarov, I. D'Amico, and H. Lowen, *Phys.Rev.Lett.* **81**, 1334 (1998).
- [203] M. Kardar and R. Golestanian, *Rev. Mod. Phys.* **71**, 1233 (1999).
- [204] N. Grønbech-Jensen, K. M. Beardmore, and P. Pincus, *Physica A* **261**, 74 (1998).
- [205] A. W. C. Lau, D. Levine, and P. Pincus, *Phys. Rev. Lett.* **84**, 4116 (2000).
- [206] F. Solis and M. de la Cruz, *Phys. Rev. E* **60**, 4496 (1999).
- [207] A. Schmidt, *J. Chem. Phys.* **110**, 113 (1999).
- [208] A. B. Schmidt, *Physica A* **293**, 21 (2001).
- [209] J. F. Stilck, Y. Levin, and J. J. Arenzon, *J. Stat. Phys.* **106**, 287 (2002).
- [210] J. Pelta and et al., *Biophys. J.* **71**, 48 (1996).
- [211] J. Pelta and et al., *J. Biol. Chem.* **271**, 5656 (1996).
- [212] M. Saminathan and et al., *Biochemistry* **38**, 3821 (1999).
- [213] T. T. Nguyen, I. Rouzina, and B. I. Shklovskii, *J. Chem. Phys.* **112**, 2562 (2000).
- [214] A. Diehl, H. A. Carmona, and Y. Levin, *Phys. Rev. E* **64**, 011804 (2001).
- [215] M. Deserno, A. Arnold, and C. Holm, cond-mat/0206126 (unpublished).
- [216] B.-Y. Ha and A. J. Liu, cond-mat/0003162 (unpublished).
- [217] B.-Y. Ha and A. J. Liu, *Europhys. Lett.* **46**, 624 (1999).
- [218] L. Belloni, *J. Phys.: Cond. Mat.* **12**, R549 (2000).
- [219] Y. Levin, *Physica A* **265**, 432 (1999).
- [220] B. Ninham and V. A. Parsegian, *J. Theoret. Biol.* **31**, 405 (1971).
- [221] S. T. Chui and J. D. Weeks, *Phys. Rev. B* **14**, 4978 (1976).
- [222] M. K. Gilson and et al., *J. Mol. Biology* **184**, 503 (1985).
- [223] R. Penfold, J. Warwicker, and B. Jonsson, *J. Phys. Chem. B* **102**, 8599 (1998).
- [224] V. Spassov and D. Bashford, *Prot. Sci.* **7**, 554 (1998).
- [225] P. Auffinger and E. Westhof, *Curr. Opin. Struc. Biol.* **8**, 227 (1998).
- [226] P. Auffinger, S. LouiseMay, and E. Westhof, *Faraday Discuss.* **103**, 151 (1996).